Snapback repellers as a cause of chaotic vibration of the wave equation with a van der Pol boundary condition and energy injection at the middle of the span

Dedicated to Professor John E. Lagnese on the occasion of his 60th birthday

Goong Chen[a)]
Department of Mathematics, Texas A&M University, College Station, Texas 77843

Sze-Bi Hsu[b)]
Department of Mathematics, National Tsing Hua University, Hsinchu, Taiwan, Republic of China

Jianxin Zhou[c)]
Department of Mathematics, Texas A&M University, College Station, Texas 77843

(Received 29 May 1998; accepted for publication 8 July 1998)

A wave equation on a one-dimensional interval I has a van der Pol type nonlinear boundary condition at the right end. At the left end, the boundary condition is fixed. At exactly the midpoint of the interval I, energy is injected into the system through a pair of transmission conditions in the feedback form of anti-damping. We wish to study chaotic wave propagation in the system. A cause of chaos by snapback repellers has been identified. These snapback repellers are repelling fixed points possessing homoclinic orbits of the non-invertible map in 2D corresponding to wave reflections and transmissions at, respectively, the boundary and the middle-of-the-span points. Existing literature [F. R. Marotto, J. Math. Anal. Appl. **63**, 199–223 (1978)] on snapback repellers contains an error. We clarify the error and give a refined theorem that snapback repellers imply chaos. Numerical simulations of chaotic vibration are also illustrated. © *1998 American Institute of Physics.* [S0022-2488(98)02012-X]

I. INTRODUCTION

Earlier, in a series of papers (Refs. 1–4), we studied chaotic vibrations of the wave equation due to a nonlinear self-excitation boundary condition of a van der Pol type: For the wave equation

$$w_{tt}(x,t)-w_{xx}(x,t)=0, \quad 0<x<1, \quad t>0, \tag{1}$$

let the right-end boundary condition be self-exciting:

$$w_x(1,t)=\alpha w_t(1,t)-\beta w_t^3(1,t), \quad \alpha,\beta>0, \quad t>0; \tag{2}$$

and let the left-end boundary condition be either fixed or free:

$$w(0,t)=0 \ \ (\text{fixed end}) \quad \text{or} \quad w_x(0,t)=0 \ \ (\text{free end}), \tag{3}$$

then the study in Refs. 2 and 4 shows that for initial conditions of generic type, the gradient (w_x,w_t) and the Riemann invariants (w_x+w_t,w_x-w_t) of (1) will be asymptotically periodic with one (for $0<\alpha\leqslant 1$) or two frequencies (for $\alpha>1$). Thus the wave equation does not have chaotic vibrations. However, instead of (3), if energy is injected into the system at the left end in the form of the boundary condition

[a)]Electronic mail: gchen@math.tamu.edu
[b)]Electronic mail: sbhsu@am.nthu.edu.tw
[c)]Electronic mail: jzhou@math.tamu.edu

$$w_x(0,t) = -\eta w_t(0,t), \quad \eta > 0, \quad \eta \neq 1. \tag{4}$$

Then for a certain parameter range of η, the injected energy will excite (asymptotically) periodic vibrations into chaos (Refs. 3 and 4). The proofs in Refs. 1 and 4 are based upon the reflection relations of the equation (1) at the two endpoints $x=0$ and $x=1$, which is perhaps the most natural Poincaré section of the initial-boundary value problem stated above.

Existing study on chaos in differential equations is concerned mostly with unpredictable behavior originating from nonlinearities appearing either in the governing equations or/and boundary conditions. Very few works have treated chaotic nonlinear systems containing disturbances or excitations from in-span or interior *pointwise sources*. So let us consider the following scenario. Let (1)–(3) stay the same as above and, in addition, assume that energy is injected into the system at an *in-span point*, say $x=a$, where $0<a<1$. This is a *pointwise excitation*. Can this also rouse periodic vibrations to chaos?

A volcanic eruption on earth may be idealized as a pointwise disturbance or excitation to the physical system governing global weather, because the scale of the volcano is negligibly small compared with that of the earth. The eruption injects ashes, chemicals, and energy, among other things, into the atmospheric currents and the stratosphere and can easily throw the global weather patterns off balance and into chaos, provided that the eruption is long and forceful. Our study undertaken here bears the resemblance of the kind of pointwise excitation occurring in Mother Nature and, thus, signifying certain mathematical and physical relevance of both models meriting investigation. However, we must also point out the dissimilarity: the volcanic eruption injects energy into the weather system as *exogenous forcing*, whereas the energy injection at an in-span point considered in this paper is in the *endogenous feedback form of anti-damping.*

We now describe the details of the mathematical model we wish to treat. Consider the wave equation

$$w_{tt}(x,t) - w_{xx}(x,t) = 0, \quad -1<x<0, \quad 0<x<1, \quad t>0. \tag{5}$$

The spatial interval is chosen to be $(-1,1)$ just for convenience. The wave speed plays a very minor role in the subsequent mathematical analysis, so we just set it to be equal to 1 in (5). Again, let the right-end boundary condition be self-exciting:

$$w_x(1,t) = \alpha w_t(1,t) - \beta w_t^3(1,t), \quad 0<\alpha \leqslant 1, \quad \beta>0, \quad t>0. \tag{6}$$

Note here that we require $0<\alpha \leqslant 1$ in order to avoid hysteresis and nonuniqueness of solutions.[2,4] At the left end, assume that the boundary condition be fixed:

$$w(-1,t) = 0, \quad t>0. \tag{7}$$

[If this is replaced by the free end boundary condition $w_x(-1,t)=0, \quad t>0$, then the mathematical analysis remains qualitatively the same.] At *exactly the middle of the span, $x=0$, we consider two types of transmission conditions:*

$$\text{(Type I)} \begin{cases} w_t(0+,t) - w_t(0-,t) = -\eta w_x(0+,t), \\ w_x(0-,t) = w_x(0+,t), \end{cases} \quad t>0, \quad \eta>0, \quad \eta \neq 2, \tag{8}$$

or

$$\text{(Type II)} \begin{cases} w(0-,t) = w(0+,t) \\ w_x(0+,t) - w_x(0-,t) = -\eta w_t(0+,t), \end{cases} \quad t>0, \quad \eta>0, \quad \eta \neq 2. \tag{8'}$$

Also prescribed are two initial conditions

$$w(x,0) = w_0(x), \quad w_t(x,0) = w_1(x), \quad -1<x<1, \tag{9}$$

where the initial state (w_0, w_1) lies in appropriate function spaces. The energy, $E(t)$, of the overall system (5)–(9), at time t, is defined to be

$$E(t)=\frac{1}{2}\int_{-1}^{1}[w_x(x,t)^2+w_t(x,t)^2]\,dx.$$

We now examine the two sets of transmission conditions (8) and (8′). Consider the time rate of change of energy:

$$\begin{aligned}\frac{d}{dt}E(t)&=\int_{-1}^{0}(w_xw_{xt}+w_tw_{tt})\,dx+\int_{0}^{1}(w_xw_{xt}+w_tw_{tt})\,dx\\&=\ldots[\text{integrating by parts and utilizing}(5)\text{–}(8')]\\&=\alpha w_t(1,t)^2-\beta w_t(1,t)^4+\begin{cases}\eta w_x(0+,t)^2 & \text{for (8)},\\ \eta w_t(0+,t)^2 & \text{for (8)}'.\end{cases}\end{aligned}\tag{10}\tag{10′}$$

We see that if $\eta<0$, then the transmission conditions (8) or (8)′ would have contributed *loss* of energy to the system. Indeed, for $\eta<0$, (8) and (8)′ model (the *only*) two primary *feedback damping* designs we know of today in structural dynamics (Ref. 5, pp. 50–51). But here in (8) or (8)′, we require $\eta>0$. Therefore the in-span conditions (8) or (8)′ contribute *energy increase* to the system. Therefore, physically, (8) or (8)′ correspond to *feedback anti-damping* devices which *inject energy* into the system.

Note that the first two terms $\alpha w_t(1,t)^2-\beta w_t(1,t)^4$, in (10) or (10)′, signify as in Refs. 2–4 the *self-regulating* (or self-exciting) effect of the boundary condition (6) because we have

$$\alpha w_t(1,t)^2-\beta w_t(1,t)^4\begin{cases}\geqslant 0 & |w_t(1,t)|\leqslant(\alpha/\beta)^{1/2},\\ \text{if} & \\ <0 & |w_t(1,t)|>(\alpha/\beta)^{1/2},\end{cases}\tag{11}\tag{11′}$$

i.e., it causes energy to *rise* if the velocity magnitude $|w_t(1,t)|$ *is small*, and to *fall* if $|w_t(1,t)|$ *is large*, just like what the damping terms do in the van der Pol ordinary differential equation $m\ddot{x}+(-\alpha\dot{x}+\beta\dot{x}^3)+kx=0$. Incidentally, the transmission conditions (81) can be incorporated into the governing equation (5) by rewriting it as

$$w_{tt}(x,t)-w_{xx}(x,t)-\eta w_t(0+,t)\,\delta(x)=0,\quad t>0,\tag{12}$$

where $\delta(x)$ is the Dirac delta distribution concentrated at $x=0$. Therefore, (8)′ does indeed correspond to a pointwise disturbance or excitation. Even though (8) also corresponds to a pointwise excitation, we do not as yet know of any similar way to incorporate (8) into the governing equation (5) through the adding of some delta functions.

The advantage of choosing the exact middle-of-the-span point $x_0=0\pm$ in (8) or (8)′ is that it makes the *method of characteristics* easily applicable to our model problem for the purpose of mathematical analysis. If, instead, we replace $x_0=0\pm$ by $x_0=a\pm$ therein, for some arbitrary a, $-1<a<1$, then the problem obviously is much more generally posed. Unfortunately, this generality (of x_0) also renders the problem highly intractable in mathematical technicality. As we will see below, the approach of the method of characteristics adopted by us is *not robust* with respect to the choice of energy injection point $x_0=0\pm$ in the sense that a slight perturbation, say, changing $x_0=0\pm$ to $x_0=\varepsilon\pm$ for some small $\varepsilon\neq 0$, would immediately fail all the mathematical analysis based on this approach. So the question is, how good or sound is the main conclusion of the paper that chaotic vibrations exist when $x_0\neq 0\pm$? This may be responded to, in a nonrigorous way, as follows. From the work in Ref. 6, we know that, in the linear case, corresponding to the choice $x_0=\varepsilon\pm$ with ε being irrational, there are many *aperiodic* solutions and, thus, the general system (with $x_0=\varepsilon\pm$) should be ''even more chaotic'' than the special case $x_0=0\pm$ when the nonlinearity (6) is present. However, a rigorous proof of this heuristic claim seems to be far out of reach for the time being; more efforts are required in order to be able to treat the general case.

We are now in a position to apply the method of characteristics to treat (5)–(9) as follows. Define, by folding the interval $(-1,0)$ onto the interval $(0,1)$, the following:

$$\left.\begin{aligned} w^{(1)}(x,t) &= -w(-x,t) \\ w^{(2)}(x,t) &= w(x,t) \end{aligned}\right\} \quad \text{for } x\in[0,1], \quad t\geqslant 0, \tag{13}$$

$$u_i=\tfrac{1}{2}(w_x^{(i)}+w_t^{(i)}), \quad v_i=\tfrac{1}{2}(w_x^{(i)}-w_t^{(i)}), \quad i=1,2. \tag{14}$$

Then the wave equation (5) is converted into a first-order hyperbolic system

$$\frac{\partial}{\partial t}\begin{bmatrix} u_1 \\ u_2 \\ v_1 \\ v_2 \end{bmatrix} = \begin{bmatrix} 1 & 0 & 0 & 0 \\ 0 & 1 & 0 & 0 \\ 0 & 0 & -1 & 0 \\ 0 & 0 & 0 & -1 \end{bmatrix} \frac{\partial}{\partial x}\begin{bmatrix} u_1 \\ u_2 \\ v_1 \\ v_2 \end{bmatrix}, \quad 0<x<1, \quad t>0. \tag{15}$$

The reflection relation at $x=1$, according to (6), (7), and (14), is

$$\begin{bmatrix} u_1(1,t) \\ u_2(1,t) \end{bmatrix} = \mathcal{R}_{1,\alpha\beta}\left(\begin{bmatrix} v_1(1,t) \\ v_2(1,t) \end{bmatrix}\right) \equiv \begin{bmatrix} v_1(1,t) \\ F_{\alpha,\beta}(v_2(1,t)) \end{bmatrix}, \tag{16}$$

where for each given $v\in\mathbb{R}$ the function $u=F_{\alpha,\beta}(v)$ is well defined through the following implicit cubic equation,[2]

$$\beta(u-v)^3+(1-\alpha)(u-v)+2v=0. \tag{17}$$

Thus (16) constitutes the right-end boundary condition for (15). In what follows, we often write $\mathcal{R}_{1,\alpha\beta}$ simply as $\mathcal{R}_1$, in case no ambiguities should occur.

Remark I.1: In (17), for given fixed α, $0<\alpha\leqslant 1$, there exists a unique $u\in\mathbb{R}$ satisfying (17) for each given $v\in\mathbb{R}$. Contrarily, if $\alpha\notin(0,1]$, i.e., $1-\alpha\notin[0,1)$, for each given $v\in\mathbb{R}$, then there may exist one, two, or three real solution(s) $u\in\mathbb{R}$, and thus $F_{\alpha,\beta}$ is no longer a well-defined function. See more in (31)–(33) below. □

The reflection (i.e., transmission) relation at $x=0$, according to (8), (8′), and (14), is, respectively,

$$\begin{bmatrix} v_1(0,t) \\ v_2(0,t) \end{bmatrix} = \mathcal{R}_{0,\eta}\left(\begin{bmatrix} u_1(0,t) \\ u_2(0,t) \end{bmatrix}\right) \equiv \begin{bmatrix} \dfrac{\eta}{2-\eta} & \dfrac{2}{2-\eta} \\ \dfrac{2}{2-\eta} & \dfrac{\eta}{2-\eta} \end{bmatrix} \begin{bmatrix} u_1(0,t) \\ u_2(0,t) \end{bmatrix} \quad \text{for (8)}; \tag{18}$$

$$\begin{bmatrix} v_1(0,t) \\ v_2(0,t) \end{bmatrix} = -\mathcal{R}_{0,\eta}\left(\begin{bmatrix} u_1(0,t) \\ u_2(0,t) \end{bmatrix}\right), \quad \text{for (8′)}. \tag{18′}$$

The above [(18) or (18′)) constitutes the left-end boundary condition for (15). From now on, we often abbreviate $\mathcal{R}_{0,\eta}$ as $\mathcal{R}_0$. By abuse of notation, we will make no distinction between $\mathcal{R}_{0,\eta}$ and the matrix on the rhs of (18).

The original initial conditions (9) now lead to

$$\begin{bmatrix} u_1(x,0) \\ u_2(x,0) \\ v_1(x,0) \\ v_2(x,0) \end{bmatrix} = \begin{bmatrix} u_{1,0}(x) \\ u_{2,0}(x) \\ v_{1,0}(x) \\ v_{2,0}(x) \end{bmatrix}, \quad 0<x<1, \tag{19}$$

for some functions $u_{i,0}(x), v_{i,0}(x), x\in(0,1), i=1,2$, according to (14). In summary, (15)–(19) constitute the complete set of a well-posed initial-boundary value problem. This system has a unique solution (u_1,u_2,v_1,v_2): for $t=2k+\tau$, $k=0,1,2,\ldots,0\leqslant\tau<2$ and $0\leqslant x\leqslant 1$,

$$\begin{bmatrix} u_1(x,t) \\ u_2(x,t) \end{bmatrix} = \begin{cases} (\mathcal{R}_1 \circ \mathcal{R}_0)^k \left(\begin{bmatrix} u_{1,0}(x+\tau) \\ u_{2,0}(x+\tau) \end{bmatrix} \right), & \tau \leqslant 1-x, \\ \mathcal{R}_0^{-1} \circ (\mathcal{R}_0 \circ \mathcal{R}_1)^{k+1} \left(\begin{bmatrix} v_{1,0}(2-x-\tau) \\ v_{2,0}(2-x-\tau) \end{bmatrix} \right), & 1-x < \tau \leqslant 2-x, \\ (\mathcal{R}_1 \circ \mathcal{R}_0)^{k+1} \left(\begin{bmatrix} u_{1,0}(\tau+x-2) \\ u_{2,0}(\tau+x-2) \end{bmatrix} \right), & 2-x < \tau \leqslant 2; \end{cases}$$

$$\begin{bmatrix} v_1(x,t) \\ v_2(x,t) \end{bmatrix} = \begin{cases} (\mathcal{R}_0 \circ \mathcal{R}_1)^k \left(\begin{bmatrix} v_{1,0}(x-\tau) \\ v_{2,0}(x,\tau) \end{bmatrix} \right), & \tau \leqslant x, \\ \mathcal{R}_0 \circ (\mathcal{R}_0 \circ \mathcal{R}_1)^k \left(\begin{bmatrix} u_{1,0}(\tau-x) \\ u_{2,0}(\tau-x) \end{bmatrix} \right), & x < \tau \leqslant 1+x, \\ (\mathcal{R}_0 \circ \mathcal{R}_1)^{k+1} \left(\begin{bmatrix} v_{1,0}(2+x-\tau) \\ v_{2,0}(2+x-\tau) \end{bmatrix} \right), & 1+x < \tau \leqslant 2, \end{cases} \tag{20}$$

which has the same form as Ref. 2, (13) and (14). In the above, all the $\mathcal{R}_0$'s may be replaced by $-\mathcal{R}_0$'s if (18′) [or, equivalently, (8′))] takes place in lieu of (18).

Naturally, from the explicit representation (20) of the solution, the system (15)–(19) manifests chaotic behavior if and only if (the iterates of) the composite map(s) $\mathcal{R}_0\mathcal{R}_1$ and/or $\mathcal{R}_1\mathcal{R}_0$ is/are chaotic. Actually, $\mathcal{R}_0\mathcal{R}_1$ and $\mathcal{R}_1\mathcal{R}_0$ have identical dynamical behavior. This is seen in the following.

Proposition I.1: For each given α, $0 < \alpha \leqslant 1$, $\beta > 0$, *and* $\eta > 0$, $\eta \neq 2$, *the maps* $\mathcal{R}_{0,\eta}\mathcal{R}_{1,\alpha\beta}$ *and* $\mathcal{R}_{1,\alpha\beta}\mathcal{R}_{0,\eta}$ *are topologically conjugate.*

Proof: First, we note that $\mathcal{R}_{0,\eta}$ is an invertible 2×2 matrix. The rest is then obvious from the following commutative diagram:

$$\begin{array}{ccc} \mathbb{R}^2 & \xrightarrow{\mathcal{R}_{0,\eta}\mathcal{R}_{1,\alpha\beta}} & \mathbb{R}^2 \\ \mathcal{R}_{0,\eta}^{-1} \downarrow & & \downarrow \mathcal{R}_{0,\eta}^{-1} \\ \mathbb{R}^2 & \xrightarrow{\mathcal{R}_{1,\alpha\beta}\mathcal{R}_{0,\eta}} & \mathbb{R}^2 \end{array}$$

□

Therefore, investigation of the periodic and chaotic behavior of only $\mathcal{R}_0\mathcal{R}_1$ suffices, because it implies that of $\mathcal{R}_1\mathcal{R}_0$, and vice versa.

If the transmission conditions (8′) take effect rather than (8), then we need to use (18′) and, consequently, (20), but with all $\mathcal{R}_0$'s therein substituted by $-\mathcal{R}_0$'s. This means that we must investigate the chaotic behavior of $-\mathcal{R}_0\mathcal{R}_1$ rather than $\mathcal{R}_0\mathcal{R}_1$. From the mathematical analysis point of view, we have found that the treatment of $-\mathcal{R}_0\mathcal{R}_1$ is qualitatively the same as that of $\mathcal{R}_0\mathcal{R}_1$. Henceforth, we will therefore only consider (8), (18), and the ensuing $\mathcal{R}_0\mathcal{R}_1$.

The main objective of this paper is to study the occurrence of chaos for the wave equation system as described. Recall from our earlier studies in Refs. 2–4 that the parameter β plays the *role of scaling*. Therefore, we may just fix β to be a positive constant, say $\beta = 1$. By varying α and η increasingly from zero, either separately or jointly, we have observed through computer simulations at least the following three routes/sources of chaos for the map $\mathcal{R}_{0,\eta}R_{1,\alpha\beta}$:

A. Period doubling

For positive α and η close to zero, the map $\mathcal{R}_{0,\eta}\mathcal{R}_{1,\alpha\beta}$ has a stable period-4 orbit in two dimensions (2D). (It does not have any period-2 orbit, according to Proposition III.5 in Sec. III below.) Let us, say, fix $\alpha = 1/2$ (and $\beta = 1$), for example. By increasing η, at $\eta \approx 0.6725$, we observe that this period-4 orbit loses stability, and a new stable period-8 orbit supersedes it. The ratios of successive differences of parametrical values η where period doublings occur have been verified to tend to Feigenbaum's constant. So the numerical evidence in support of period doubling is strong and beyond doubt. Nevertheless, at this moment, the authors are only partially successful in establishing a period-doubling bifurcation theorem in 2D and in carrying out a computer-aided verification of the theorem. We hope to be able to defer a complete presentation of this to a sequel.

B. Snapback repellers

These are repelling fixed points or periodic points in whose neighborhoods a homoclinic orbit originates. For example (see Example V.1 in Sec. V), the origin in $\mathbb{R}^2$, as a repelling fixed point, is a snapback repeller for a restricted range of α and η values. So far, this is the only case for which we have sufficient understanding; its discussion will be the focus of the study in this paper (see more in Secs. IV and V).

C. Nondiffeomorphic horseshoes

The Smale horseshoe is a powerful technique for proving chaos of multidimensional maps. However, the powerful Smale–Birkhoff homoclinic theorem (Ref. 7, pp. 482–483) requires that the map be a *diffeomorphism*; so it must at least be *invertible*. Ours is not the case here because $\mathcal{R}_{1,\alpha\beta}$ is not invertible for any α, $0<\alpha\leqslant 1$, $\beta>0$; see Remark I.1 and (31)–(33) below. The lack of invertibility of $\mathcal{R}_1$ and, consequently, of $\mathcal{R}_0\mathcal{R}_1$ is related to the prevalent *irreversible* behavior of time-dependent nonlinear PDEs; see Sec. II. Numerical evidence strongly suggests that the map $\mathcal{R}_0\mathcal{R}_1$ has many periodic points of *saddle node* type in whose neighborhoods homoclinic orbits originate and, thus, we speculate that they cause chaos. (For lack of a better term, we call this a ''non-diffeomorphic horseshoe'' for the time being.) See some details in Example V.2. Notwithstanding, we must concede that before a rigorous proof is given, this remains just a speculation. For general non-invertible maps in two- or higher-dimensional spaces, as pointed out by Mira *et al.*[8] there are *not many optional* theoretical methods available to rigorously prove the occurrence of chaos. More dedicated cultivation of this area is very desirable.

The organization of the paper proceeds as follows. In Sec. II, we discuss the time irreversibility of our PDE system. In Sec. III, elementary properties of the map, including fixed points, stability, and invariant domains, are studied. In Sec. IV, we study chaos caused by snapback repellers. We point out an error in an earlier work by Marotto[9] and give a refined proof. In Sec. V, we present examples and illustrations of chaotic vibrations.

II. IRREVERSIBILITY FOR NONLINEAR PARTIAL DIFFERENTIAL EQUATIONS: THE LACK OF DIFFEOMORPHISM TO FORM A SMALE HORSESHOE

Recall from Ref. 2 that for $0<\alpha\leqslant 1$, $\beta>0$, the implicit relation (17) determines a unique function $u=F(v)=F_{\alpha,\beta}(v)$, where

$$u=F(v)=v+\left[-\frac{v}{\beta}+\sqrt{\frac{1}{27}\left(\frac{1-\alpha}{\beta}\right)^3+\frac{v^2}{\beta^2}}\right]^{1/3}+\left[-\frac{v}{\beta}-\sqrt{\frac{1}{27}\left(\frac{1-\alpha}{\beta}\right)^3+\frac{v^2}{\beta^2}}\right]^{1/3}, \tag{21}$$

by Cardan's formula. The function F is odd, with two critical points—one maximum and one minimum—at, respectively $-v_c^*$ and v_c^*, where $v_c^*=[(2-\alpha)/3]\sqrt{(1+\alpha)/3\beta}$. We also know that F satisfies the following properties:

$$\text{(i)}\quad F'(0)=-\frac{1+\alpha}{1-\alpha}, \tag{22}$$

$$\text{(ii)}\quad 0<F'(v)<1 \quad \text{for } |v|>v_c^*; \tag{23}$$

$$\text{(iii)}\quad F \text{ has three intercepts at } v=-v_I,\ 0,\ v_I, \quad \text{where } v_I\equiv\sqrt{\frac{1+\alpha}{\beta}}. \tag{24}$$

Also, recall from Ref. 3 that for η, $0<\eta<1$, the map $u=G\circ F(v)=G_\eta\circ F_{\alpha,\beta}(v)$, where $G_\eta\equiv(1+\eta)/(1-\eta)$, has exactly three fixed points

$$v=G\circ F(v), \quad \text{for } v=-v^*,\ 0,\ v^*; \quad v^*\equiv\frac{1+\eta}{2\eta}\sqrt{\frac{1+\alpha\eta}{\beta\eta}}. \tag{25}$$

Now, let us consider the question whether the system (15)–(19) is *time reversible*. We make a change of variable $t\mapsto -t$ and consider $t\geqslant 0$; we obtain the time-reversed system

$$\frac{\partial}{\partial t}\begin{bmatrix}\tilde{u}_1\\ \tilde{u}_2\\ \tilde{v}_1\\ \tilde{v}_2\end{bmatrix}=\begin{bmatrix}1&0&0&0\\0&1&0&0\\0&0&-1&0\\0&0&0&-1\end{bmatrix}\frac{\partial}{\partial x}\begin{bmatrix}\tilde{u}_1\\ \tilde{u}_2\\ \tilde{v}_1\\ \tilde{v}_2\end{bmatrix},\quad 0<x<1,\quad t>0, \tag{26}$$

with boundary conditions

$$\text{at } x=0\begin{bmatrix}\tilde{v}_1(0,t)\\ \tilde{v}_2(0,t)\end{bmatrix}=\tilde{\mathcal{R}}_0\left(\begin{bmatrix}\tilde{u}_1(0,t)\\ \tilde{u}_2(0,t)\end{bmatrix}\right)=\begin{bmatrix}-\frac{\eta}{2+\eta}&\frac{2}{2+\eta}\\ \frac{2}{2+\eta}&-\frac{\eta}{2+\eta}\end{bmatrix}\begin{bmatrix}\tilde{u}_1(0,t)\\ \tilde{u}_2(0,t)\end{bmatrix},\quad t>0,\quad (\eta>0), \tag{27}$$

$$\text{at } x=1\begin{bmatrix}u_1(1,t)\\ u_2(1,t)\end{bmatrix}=\tilde{\mathcal{R}}_1\left(\begin{bmatrix}\tilde{v}_1(1,t)\\ \tilde{v}_2(1,t)\end{bmatrix}\right)=\begin{bmatrix}\tilde{v}_1(1,t)\\ \tilde{F}_{\alpha,\beta}(\tilde{v}_2(1,t)\end{bmatrix},\quad t>0, \tag{28}$$

and certain initial conditions

$$\tilde{u}_i(x,0)=\tilde{u}_{i,0}(x),\quad \tilde{v}_i(x,0)=\tilde{v}_{i,0}(x),\quad i=1,2,\quad x\in[0,1], \tag{29}$$

where, in (28), the relation $\tilde{u}=\tilde{F}_{\alpha,\beta}(\tilde{v})$ is defined through the following cubic equation:

$$\beta(\tilde{u}-\tilde{v})^3-(1+\alpha)(\tilde{u}-\tilde{v})-2\tilde{v}=0,\quad 0<\alpha\leqslant 1,\quad \beta>0. \tag{30}$$

Note that $\tilde{u}$ and $\tilde{v}$ are restricted to be reals in (30). The relation $\tilde{F}_{\alpha,\beta}$ is *not* a function, as Cardan's formula for cubic algebraic equations gives the solutions of (30) as follows: let

$$D(\tilde{v})\equiv-\frac{1}{27}\frac{(1+\alpha)^3}{\beta^3}+\frac{\tilde{v}^2}{\beta^2}$$

be the discriminant for (30). Then
(i) if $D(\tilde{v})>0$, then $\tilde{u}$ is uniquely determined by $\tilde{v}$:

$$\tilde{u}=\tilde{F}_{\alpha,\beta}(\tilde{v})=\tilde{v}+\left[-\frac{\tilde{v}}{\beta}+\sqrt{D(\tilde{v})}\right]^{1/3}+\left[-\frac{\tilde{v}}{\beta}-\sqrt{D(\tilde{v})}\right]^{1/3}, \tag{31}$$

(ii) If $D(\tilde{v})<0$, then (30) yields three real solutions:

$$\tilde{u}_k=2S\ \cos\frac{\phi+2k\pi}{3};\quad S\equiv\sqrt{\frac{1}{3}\frac{1+\alpha}{\beta}},\quad \phi\equiv\cos^{-1}\left[\frac{3\sqrt{3}\tilde{v}}{(1+\alpha)}\sqrt{\frac{\beta}{1+\alpha}}\right],\quad k=1,2,3. \tag{32}$$

(iii) If $D(\tilde{v})=0$, then (30) yields two distinct real solutions:

$$\tilde{u}_1=2\sqrt[3]{\frac{\tilde{v}}{\beta}},\quad \tilde{u}_2=\sqrt[3]{-\frac{\tilde{v}}{\beta}}\ \text{(with multiplicity 2)}. \tag{33}$$

The multiplicity of solutions given in (32) and (33) spells trouble for the system (26)–(29). We have the following.

Theorem II.1 [Lack of global irreversibility of the system (15)–(19)]: *Let (26)–(29) be the time-reversed system of (15)–(19). Assume that the initial conditions* $\tilde{u}_{i,0}(x),\tilde{v}_{i,0}(x)$, $i=1,2$, *in (29) are continuous functions on [0,1] such that not all of these functions are identically zero. Then there exists an* $\varepsilon>0$ *such that if*

$$0 \leqslant \inf_{x\in[0,1]} |\tilde{u}_{i,0}(x)| < \varepsilon, \quad \text{or} \quad 0 \leqslant \inf_{x\in[0,1]} |\tilde{v}_{i,0}(x)| < \varepsilon, \quad \text{for some } i=1 \text{ or } 2,$$

then the solution of the system (26)–(29) is not unique for $t>T$, for some $T>0$.

Proof: If $\tilde{v}_{2,0}(x) \not\equiv 0$, and if there exists some $\xi \in (0,1)$ such that

$$|\tilde{v}_{2,0}(\xi)| \leqslant \frac{1+\alpha}{3\sqrt{3}} \sqrt{\frac{1+\alpha}{\beta}}, \tag{34}$$

then $D(\tilde{v}_{2,0}(\xi)) \leqslant 0$. By (32) or (33), after the reflection at $x=1$ takes place at time $t=1-\xi$ through the relation (28), we see that the $\tilde{u}_2$-component lacks uniqueness. Therefore the solution of the system (26)–(29) loses uniqueness after $T=1-\xi$.

If $\tilde{v}_{2,0}(x) \equiv 0$ or if (34) does not hold for any $\xi \in (0,1)$, then there exists some $\xi \in (0,1)$ such that one of the following,

$$0 < |\tilde{u}_{1,0}(\xi)| < \varepsilon, \quad 0 < |\tilde{u}_{2,0}(\xi)| < \varepsilon, \quad 0 < |\tilde{v}_{1,0}(\xi)| < \varepsilon, \tag{35}$$

is true. We note that at $x=0$ the reflection matrix $\tilde{\mathcal{R}}_0$ has two eigenvalues: -1 and $(2-\eta)/(2+\eta)$, both with magnitudes not larger than 1. Thus $\tilde{\mathcal{R}}_0$ is nonexpansive. By choosing ε sufficiently small and tracing reflections along characteristics, by using the nonexpansiveness of $\tilde{\mathcal{R}}_0$ plus some detailed arguments (which are omitted), we obtain from (20) that at some $t_0>0$, we will gain

$$|\tilde{v}_2(\tilde{\xi},t_0)| \leqslant \frac{1+\alpha}{3\sqrt{3}} \sqrt{\frac{1+\alpha}{\beta}}, \quad \text{for some } \tilde{\xi} \in (0,1).$$

Therefore again (32) or (33) applies, and, by (28), the solution loses uniqueness. □

The above irreversible behavior has all but ruled out the direct applicability of Smale's horseshoe to our problem.

III. ELEMENTARY PROPERTIES OF THE MAP $\mathcal{R}_0\mathcal{R}_1$

In this section, we perform an elementary stability analysis of fixed points of $\mathcal{R}_0\mathcal{R}_1$ and determine some invariant regions.

Proposition III.1: Let $0<\alpha\leqslant 1$, $\beta \geqslant 1$, and $\eta>0, \eta\neq 2$. Then the map $\mathcal{R}_0\mathcal{R}_1$ has exactly three fixed points:

$$(0,0), (v_1^*, v_2^*) \equiv \left(\frac{1}{2\eta}\sqrt{\frac{1+\alpha\eta}{\beta\eta}}, \frac{1+\eta}{2\eta}\sqrt{\frac{1+\alpha\eta}{\beta\eta}} \right), \quad (-v_1^*, -v_2^*). \tag{36}$$

Proof: We determine the fixed points by solving

$$\begin{bmatrix} v_1 \\ v_2 \end{bmatrix} = \mathcal{R}_0\mathcal{R}_1 \left(\begin{bmatrix} v_1 \\ v_2 \end{bmatrix} \right) = \begin{bmatrix} \dfrac{\eta}{2-\eta} v_1 + \dfrac{2}{2-\eta} F(v_2) \\ \dfrac{2}{2-\eta} v_1 + \dfrac{\eta}{2-\eta} F(v_2) \end{bmatrix}. \tag{37}$$

From the first component equation in (37), we obtain

$$v_1 = \frac{F(v_2)}{1-\eta}, \quad \eta \neq 1, \tag{38a}$$

$$F(v_2) = 0, \quad \eta = 1. \tag{38b}$$

For $\eta \neq 1$, substituting $(38a)_1$ into the second component equation of (37), we obtain

$$v_2=\frac{1+\eta}{1-\eta}F(v_2). \tag{39}$$

However, in the notation of Ref. 3, (2.1), (39) says exactly that $v_2=G\circ F(v_2)$, i.e., v_2 is a fixed point of the 1D map $G\circ F$, which according to (25) and (39) gives three values of v_2:

$$v_2=0,\quad \frac{1+\eta}{2\eta}\sqrt{\frac{1+\alpha\eta}{\beta\eta}},\quad -\frac{1+\eta}{2\eta}\sqrt{\frac{1+\alpha\eta}{\beta\eta}}. \tag{40}$$

Substituting these values first into (39) to obtain $F(v_2)$ and next into (38a), we obtain (36).

For $\eta=1$, (38b) says that v_2 is a v-axis intercept of F. By (24), there are three intercepts:

$$v_2=0,\quad \sqrt{\frac{1+\alpha}{\beta}},\quad -\sqrt{\frac{1+\alpha}{\beta}}. \tag{41}$$

Using these values and (38b) in the second component equation of (37), we obtain $v_1=v_2/2$. Thus we again have (36) with η being set to 1 therein. □

For any differentiable map $\mathcal{F}$: $\mathbb{R}^N\to\mathbb{R}^N$, we let $D\mathcal{F}(x)$ denote the Jacobian matrix of $\mathcal{F}$ at x. For our map $\mathcal{R}_0\mathcal{R}_1$, we have

$$D(\mathcal{R}_0\mathcal{R}_1)(v_1,v_2)=\begin{bmatrix}\frac{\eta}{2-\eta} & \frac{2}{2-\eta}F'(v_2)\\ \frac{2}{2-\eta} & \frac{\eta}{2-\eta}F'(v_2)\end{bmatrix}. \tag{42}$$

The stability analysis of fixed points and periodic points is well known to be important in the understanding of the dynamics of the map $\mathcal{R}_0\mathcal{R}_1$. We perform such an analysis for the three fixed points given in Proposition III.1.

Proposition III.2: Let $0<\alpha\leqslant 1,\beta>0$, and $0<\eta<2$. The fixed point (0,0) is a repelling fixed point of $\mathcal{R}_0\mathcal{R}_1$.

Proof: First, note from Ref. 2, Sec. III, (P. 3), that $F'(0)=-(1+\alpha)/(1-\alpha)$. From (42), we get

$$J\equiv D(\mathcal{R}_0\mathcal{R}_1)(0,0)=\begin{bmatrix}\frac{\eta}{2-\eta} & -\frac{2}{2-\eta}\frac{1+\alpha}{1-\alpha}\\ \frac{2}{2-\eta} & -\frac{\eta}{2-\eta}\frac{1+\alpha}{1-\alpha}\end{bmatrix}. \tag{43}$$

The eigenvalues of J are computed from

$$0=\det(\lambda I_2-J)\quad (\det\equiv\text{determinant})=\lambda^2-\left(1-\frac{1+\alpha}{1-\alpha}\right)\frac{\eta}{2-\eta}\lambda-\frac{1+\alpha}{1-\alpha}\left[\left(\frac{\eta}{2-\eta}\right)^2-\left(\frac{2}{2-\eta}\right)^2\right],$$

which are

$$\lambda_1,\lambda_2=\frac{1}{2}\left[-\frac{2\alpha}{1-\alpha}\frac{\eta}{2-\eta}\pm\sqrt{\left(\frac{2\alpha}{1-\alpha}\frac{\eta}{2-\eta}\right)^2-\frac{4(1+\alpha)}{1-\alpha}\frac{2+\eta}{2-\eta}}\right], \tag{44}$$

$$(\text{``}+\text{''}\quad\text{for}\ \lambda_1,\text{``}-\text{''}\text{for}\lambda_2).$$

If the discriminant Δ is negative,

$$\Delta\equiv\left(\frac{2\alpha}{1-\alpha}\frac{\eta}{2-\eta}\right)^2-\frac{4(1+\alpha)}{1-\alpha}\frac{2+\eta}{2-\eta}<0, \tag{45}$$

which happens if

$$\eta^2-4(1-\alpha^2)<0, \tag{46}$$

then λ_1 and λ_2 are complex conjugates of each other and, for $0<\eta<2$,

$$|\lambda_1|^2=|\lambda_2|^2=\lambda_1\lambda_2=-\frac{1+\alpha}{1-\alpha}\left[\left(\frac{\eta}{2-\eta}\right)^2-\left(\frac{2}{2-\eta}\right)^2\right]=\frac{1+\alpha}{1-\alpha}\frac{2+\eta}{2-\eta}>1.$$

Therefore the origin is a repelling *spiral point*.

On the other hand, if $\Delta\geqslant 0$, then $\lambda_2<\lambda_1<0$. We now show that $\lambda_1<-1$, or, from (44),

$$-\frac{2\alpha}{1-\alpha}\frac{\eta}{2-\eta}+\sqrt{\left(\frac{2\alpha}{1-\alpha}\frac{\eta}{2-\eta}\right)^2-\frac{4(1+\alpha)}{1-\alpha}\frac{2+\eta}{2-\eta}}<-2,$$

or

$$\sqrt{\left(\frac{2\alpha}{1-\alpha}\frac{\eta}{2-\eta}\right)^2-\frac{4(1+\alpha)}{1-\alpha}\frac{2+\eta}{2-\eta}}<-2+\frac{2\alpha}{1-\alpha}\frac{\eta}{2-\eta}. \tag{47}$$

Note that the rhs of the inequality above is non-negative because

$$\Delta\geqslant 0\Rightarrow\alpha^2+\frac{\eta^2}{2^2}\geqslant 1\Rightarrow\alpha+\frac{\eta}{2}\geqslant\left(\alpha^2+\frac{\eta^2}{2^2}\right)^{1/2}\geqslant 1 \quad \text{for } \alpha>0, \quad \eta>0$$

$$\Rightarrow 2\alpha+\eta-2\geqslant 0\Rightarrow -2+\frac{2\alpha}{1-\alpha}\frac{\eta}{2-\eta}\geqslant 0 \quad \text{for } 0<\alpha<1, \quad 0<\eta<2.$$

Squaring both sides of (47), we see that $\lambda_1<-1$ if and only if

$$-\frac{4(1+\alpha)}{1-\alpha}\cdot\frac{2}{2-\eta}<8, \quad \text{for } 0<\alpha<1, \quad 0<\eta<2,$$

which is always valid. Therefore $\lambda_2<\lambda_1<-1$. □

Corollary III.1: Let $0<\alpha\leqslant 1, \beta>0$, *and* $0<\eta<2$. *Then*

(i) if $\eta^2-4(1-\alpha^2)<0$, *then* (0,0) *is a repelling spiral point of* $\mathcal{R}_0\mathcal{R}_1$.

(ii) if $\eta^2-4(1-\alpha^2)\geqslant 0$, *then* (0,0) *is a repelling (star) nodal point of* $\mathcal{R}_0\mathcal{R}_1$. □

Proposition III.3: Let $0<\alpha\leqslant 1, \beta>1$, *and* $0<\eta<2$. *Then the fixed points* (v_1^*, v_2^*) *and* $(-v_1^*, -v_2^*)$ *are unstable saddle nodes of* $\mathcal{R}_0\mathcal{R}_1$.

Proof: We need only consider the stability of (v_1^*, v_2^*); that of $(-v_1^*, -v_2^*)$ follows from a symmetry argument.

The Jacobian matrix at (v_1^*, v_2^*), by (42), is

$$J\equiv\begin{bmatrix}\frac{\eta}{2-\eta} & \frac{2}{2-\eta}F'(v_2^*)\\ \frac{2}{2-\eta} & \frac{\eta}{2-\eta}F'(v_2^*)\end{bmatrix}.$$

The eigenvalues λ_1 and λ_2 of J satisfy

$$\begin{aligned}0&=\det(\lambda I_2-B)=\lambda^2-\frac{\eta}{2-\eta}(1+F'(v_2^*))-\frac{2+\eta}{2-\eta}F'(v_2^*),\\ \lambda_1,\lambda_2&=\frac{1}{2}\left[\frac{\eta}{2-\eta}(1+F'(v_2^*))\pm\sqrt{\left(\frac{\eta}{2-\eta}\right)^2(1+F'(v_2^*))^2+4\cdot\frac{2+\eta}{2-\eta}F'(v_2^*)}\right],\\ &(\text{``}+\text{''} \text{ for } \lambda_1, \quad \text{``}-\text{''} \text{ for } \lambda_2).\end{aligned} \tag{48}$$

From (22), (23), and Ref. 3, Lemma 2.4, we have

$$0<F'(v_2^*)<1, \quad \frac{1+\eta}{1-\eta}F'(v_2^*)>1. \tag{49}$$

Therefore we have $\lambda_1>0$, $\lambda_2>0$. We want to show further that

$$\lambda_1>1, \quad -1<\lambda_2<0. \tag{50}$$

From (48), we see that $\lambda_1>1$ holds if and only if

$$\sqrt{\left(\frac{\eta}{2-\eta}\right)^2(1+F'(v_2^*))^2+4\cdot\frac{2+\eta}{2-\eta}F'(v^*)}>2-\frac{\eta}{2-\eta}(1+F'(v_2^*)). \tag{51}$$

If $2-[\eta/(2-\eta)](1+F'(v_2^*))\leqslant 0$, then (51) automatically holds. So we consider $2-[\eta/(2-\eta)](1+F'(v_2^*))>0$. Squaring both sides of (51) and simplifying yields

$$\lambda_1>0\Leftrightarrow 4\cdot\frac{2+\eta}{2-\eta}F'(v_2^*)>4-\frac{4\eta}{2-\eta}(1+F'(v_2^*)),$$

$$\Leftrightarrow F'(v_2^*)>\frac{1-\eta}{1+\eta},$$

which holds by (49).

Next, we show that $0>\lambda_2>-1$. From (48),

$$\lambda_2>-1\Leftrightarrow 2+\frac{\eta}{2-\eta}(1+F'(v_2^*))>\sqrt{\left(\frac{\eta}{2-\eta}\right)^2(1+F'(v_2^*))^2+4\cdot\frac{2+\eta}{2-\eta}F'(v_2^*)}. \tag{52}$$

Squaring both sides of (52) and simplifying yields

$$\frac{4\eta}{2-\eta}(1+F'(v_2^*))+4>4\cdot\frac{2+\eta}{2-\eta}F'(v_2^*),$$

$$F'(v_2^*)<1.$$

The above again is true by (23). Therefore $\lambda_2>-1$. □

We now determine an elementary invariant rectangle, for positive η which is close to 0.

Proposition III.4: Assume $0<\alpha\leqslant 1,\beta>0$, *and* $0<\eta<1$. *Let* $G=G_\eta, F=F_{\alpha,\beta}$, v^*, v_I *and* v_c^* *be defined as in* (22)–(25). *Assume that* $\eta_{\alpha,\beta}^*$ *satisfies*

$$G_{\eta_{\alpha,\beta}^*}F_{\alpha,\beta}(-v_c^*)\leqslant v^*. \tag{53}$$

Then for η, $0<\eta<\eta_{\alpha,\beta}^*$,

$$D=\{(v_1,v_2)\in\mathbb{R}^2 \,|\, |v_1|\leqslant v_1^*, |v_2|\leqslant v_2^*\} \tag{54}$$

is invariant under $\mathcal{R}_0\mathcal{R}_1$, *i.e.,* $\mathcal{R}_0\mathcal{R}_1(D)\subset D$, *where*

$$v_1^*\equiv\frac{v^*}{1+\eta}, \quad v_2^*\equiv v^*. \tag{55}$$

Proof: Let $(v_1,v_2)\in D$ and

$$\begin{bmatrix} u_1 \\ u_2 \end{bmatrix} = \mathcal{R}_0\mathcal{R}_1\left(\begin{bmatrix} v_1 \\ v_2 \end{bmatrix}\right) = \begin{bmatrix} \frac{\eta}{2-\eta}v_1 + \frac{2}{2-\eta}F(v_2) \\ \frac{2}{2-\eta}v_1 + \frac{\eta}{2-\eta}F(v_2) \end{bmatrix}. \tag{56}$$

We want to show that $(u_1,u_2)\in D$.

By (25) and (53), using Ref. 3, Lemma 2.5, we first note that $\mathcal{I}\equiv[-v^*,v^*]$ is an invariant interval of $G\circ F$. So we have

$$-v_2^* \leqslant \frac{1+\eta}{1-\eta}F(v_2) \leqslant v_2^*, \quad \text{for all } v_2, |v_2| \leqslant v_2^* = v^*. \tag{57}$$

Thus, for $v_1, |v_1| \leqslant v_1^*$,

$$u_1 = \frac{\eta}{2-\eta}v_1 + \frac{2}{2-\eta}F(v_2) \leqslant \frac{\eta}{2-\eta}v_1^* + \frac{2}{2-\eta}F(v_2).$$

However,

$$\frac{\eta}{2-\eta}v_1^* + \frac{2}{2-\eta}F(v_2) \leqslant v_1^* \Leftrightarrow \frac{2}{2-\eta}F(v_2) \leqslant \frac{2(1-\eta)}{2-\eta}v_1^* \Leftrightarrow \frac{1+\eta}{1-\eta}F(v_2) \leqslant v_2^*. \tag{58}$$

By (57) we know that the last inequality in (58) holds. Therefore

$$u_2 \leqslant v_1^*. \tag{59}$$

Next,

$$u_1 = \frac{\eta}{2-\eta}v_1 + \frac{2}{2-\eta}F(v_2) \geqslant -\frac{\eta}{2-\eta}v_1^* + \frac{2}{2-\eta}F(v_2).$$

We have

$$\begin{aligned} -\frac{\eta}{2-\eta}v_1^* + \frac{2}{2-\eta}F(v_2) \geqslant -v_1^* &\Leftrightarrow \frac{2}{2-\eta}F(v_2) \\ &\geqslant \frac{(-2)(1-\eta)}{2-\eta}v_1^* \Leftrightarrow \frac{1+\eta}{1-\eta}F(v_2) \\ &\geqslant -(1+\eta)v_1^* \\ &= -v_2^* \Leftrightarrow \frac{1+\eta}{1-\eta}F(v_2) \geqslant -v_2^*. \end{aligned} \tag{60}$$

By (57), we again know that the last inequality in (60) holds. Hence $u_1 \geqslant -v_1^*$, which, incorporated with (59), gives $|u_1| \leqslant v_1^*$.

The proof that u_2 satisfies $|u_2| \leqslant v_2^*$ is similar and therefore omitted. □

Example III.1:

By Ref. 3, (2.20), and (25), we can determine $\eta_{\alpha,\beta}^*$ from the equality

$$G_{\eta_{\alpha,\beta}^*}F_{\alpha,\beta}(-v_c^*) = \frac{1+\eta_{\alpha,\beta}^*}{1-\eta_{\alpha,\beta}^*}\frac{1+\alpha}{3}\sqrt{\frac{1+\alpha}{3\beta}} = v^* = \frac{1+\eta_{\alpha,\beta}^*}{2\eta_{\alpha,\beta}^*}\sqrt{\frac{1+\alpha\eta_{\alpha,\beta}^*}{\beta\eta_{\alpha,\beta}^*}}.$$

Let $\alpha = 1/2$, $\beta = 1$, for example; we have

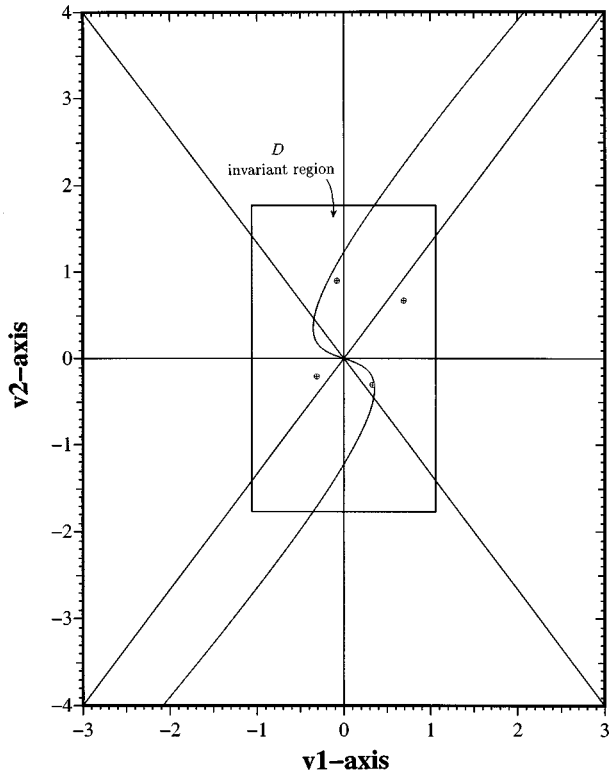

FIG. 1. An attracting period-4 orbit for Example III.1, where $\alpha=1/2$, $\beta=1$, and $\eta=2/3$ are used. The square is an invariant region guaranteed by Proposition III.4.

$$v_c^*\approx 0.3536,\ v^*\approx 1.7678 \quad \text{and} \quad \eta^*_{\alpha,\beta}=2/3\approx 0.6667,$$

$$v_1^*\approx 1.0607, \quad v_2^*=v^*\approx 1.7678.$$

For these values of α, β, and $\eta^*_{\alpha,\beta}$, we use the computer to plot the orbit $(\mathcal{R}_0\mathcal{R}_1)^k P_0$, with $P_0=(0.005,0.005)$ and $10^4\leqslant k\leqslant 10^5$. What we obtain is just an attracting period-4 orbit as shown in Fig. 1. There is another attracting period-4 orbit which is symmetric with respect to the origin of the one shown in Fig. 1 but not plotted there. □

The following can be verified in a straightforward way; its proof is omitted.

Proposition III.5: For given $\alpha, 0<\alpha\leqslant 1$, $\beta>0$, and $\eta>0, \eta\neq 2$, *the map* $\mathcal{R}_0\mathcal{R}_1$ *does not have any prime period-2 points.* □

The following theorem gives two unbounded invariant domains whereupon all trajectories grow unbounded.

Theorem III.1: Let $0<\alpha\leqslant 1$, $\beta>0$, *and* $0<\eta<1$. *Then the following two sets,*

$$U_1=\{(v_1,v_2)\in\mathbb{R}^2 | v_1\geqslant v_1^*, v_2\geqslant v_2^*\},$$

$$U_2=-U_1=\{(v_1,v_2)\in\mathbb{R}^2 | (-v_1,-v_2)\in U_1\},$$

are invariant under $\mathcal{R}_0\mathcal{R}_1$. *Furthermore, for each point* $(v_1,v_2)\in U_1\backslash\{(v_1^*,v_2^*)\}$ *we have*

$$\lim_{n\to\infty}|(\mathcal{R}_0\mathcal{R}_1)^n(v_1,v_2)|_2=\infty, \tag{61}$$

where $||_2$ is the Euclidean norm in $\mathbb{R}^2$. Same for U_2.

Proof: Let $(v_1,v_2)\in U_1$ and $(u_1,u_2)\in\mathcal{R}_0\mathcal{R}_1(v_1,v_2)$. Then

$$
\begin{aligned}
u_1 &= \frac{\eta}{2-\eta} v_1 + \frac{2}{2-\eta} F(v_2) \\
&\geqslant \frac{\eta}{2-\eta} v_1^* + \frac{2}{2-\eta} F(v_2^*) \\
&= \frac{\eta}{2-\eta} v_1^* + \frac{2}{2-\eta} \cdot \frac{1-\eta}{1+\eta} v_2^* \quad \text{[by (25),(55)]} \\
&= \left[\frac{\eta}{2-\eta} + \frac{2}{2-\eta} \cdot \frac{1-\eta}{1+\eta} \cdot (1+\eta) \right] v_1^* = v_1^*, \quad \text{[by (55)];}
\end{aligned}
$$

$$
\begin{aligned}
u_2 &= \frac{2}{2-\eta} v_1 + \frac{\eta}{2-\eta} F(v_2) \\
&\geqslant \frac{2}{2-\eta} v_1^* + \frac{\eta}{2-\eta} F(v_2^*) \\
&= \left[\frac{2}{2-\eta} \cdot \frac{1}{1+\eta} + \frac{\eta}{2-\eta} \frac{1-\eta}{1+\eta} \right] v_2^* = v_2^* \quad \text{[by (25),(55)].}
\end{aligned}
$$

Therefore U_1 is invariant under $\mathcal{R}_0\mathcal{R}_1$. The invariance of U_2 follows immediately from the oddness of the map $\mathcal{R}_0\mathcal{R}_1$.

For any initial state $(v_1^{(0)}, v_2^{(0)}) \in U_1$, let $(v_1^{(n)}, v_2^{(n)}) = (\mathcal{R}_0\mathcal{R}_1)^n (v_1^{(0)}, v_2^{(0)})$ be the nth iterate. Define the following Liapunov function on U_1:

$$
W(v_1, v_2) = \delta v_1 + v_2, \quad \text{for some } \delta > 0.
$$

Then

$$
\begin{aligned}
\Delta_1 W &\equiv W(v_1^{(1)}, v_2^{(1)}) - W(v_1^{(0)}, v_2^{(0)}) \\
&= (\delta v_1^{(1)} + v_2^{(1)}) - (\delta v_1^{(0)} + v_2^{(0)}) \\
&= \delta \left[\frac{\eta}{2-\eta} v_1^{(0)} + \frac{2}{2-\eta} F(v_2^{(0)}) \right] \\
&\quad + \left[\frac{2}{2-\eta} v_1^{(0)} + \frac{\eta}{2-\eta} F(v_2^{(0)}) \right] - (\delta v_1^{(0)} + v_2^{(0)}) \\
&= \left(\frac{\delta\eta + 2}{2-\eta} - \delta \right) v_1 + \left(\frac{2\delta + \eta}{2-\eta} F(v_2) - v_2 \right). \qquad (62)
\end{aligned}
$$

Now choose $\delta = 1/(1-\eta)$. Then $(\delta\eta + 2)/(2-\eta) - \delta = 0$, and

$$
\frac{2\delta + \eta}{2-\eta} = \frac{1+\eta}{1-\eta}.
$$

Continuing from (62), we get

$$
\Delta_1 W = \frac{1+\eta}{1-\eta} F(v_2^{(0)}) - v_2^{(0)} \geqslant 0, \quad \text{for } v_2 \geqslant v_2^*. \qquad (63)
$$

Note that equality in (63) holds when and only when $v_2 = v_2^*$. However, if $v_1^{(0)} > v_1^*$, $v_2^{(0)} = v_2^*$, then

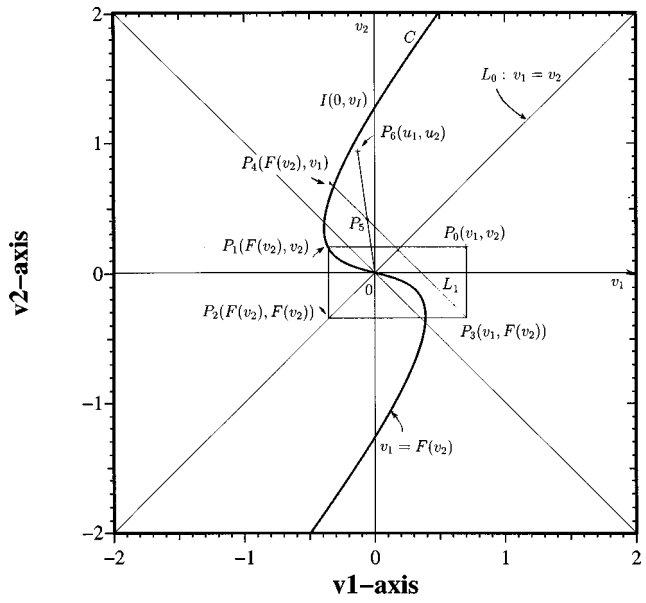

FIG. 2. Graphical construction of $(u_1,u_2)=\mathcal{R}_0\mathcal{R}_1(v_1,v_2)$.

$$v_2^{(1)}=\frac{2}{2-\eta}v_1^{(0)}+\frac{\eta}{2-\eta}F(v_2^*)>\frac{\eta}{2-\eta}v_1^*+\frac{\eta}{2-\eta}\frac{1-\eta}{1+\eta}v_2^*$$
$$=\left(\frac{2}{2-\eta}\frac{1}{1+\eta}+\frac{\eta}{2-\eta}\frac{1-\eta}{1+\eta}\right)v_2^*=v_2^*.$$

Therefore $\Delta_1 W>0$ for $(v_1^{(0)},v_2^{(0)})\in U_1\setminus\{(v_1^*,v_2^*)\}$. A little more elaborate argument further shows that $W(v_1^{(n)},v_2^{(n)})\to\infty$ as $n\to\infty$. Details are omitted. We therefore have (61). □

Remark III.1: By Theorem III.1, clearly chaos will not occur in U_1 and U_2 because trajectories originating or passing therein grow unbounded. This information is rather useful in eliminating nonchaotic cases.

Then, will chaos occur in the bounded invariant rectangle D in (53) for η in the range $0<\eta<\eta^*_{\alpha,\beta}$? Through numerical experiments, we have found that the answer is also negative; the map $\mathcal{R}_0\mathcal{R}_1$ displays only periodic behavior with periods 2^n, i.e., for the parameter range $\eta, 0<\eta<\eta^*_{\alpha,\beta}$, all orbits are asymptotically periodic; see Example III.1. What we have found empirically is that strange attractors (invariant regions) for chaotic $\mathcal{R}_0\mathcal{R}_1$ consist mainly of points in D, plus a small portion of points lying *outside* $D\cup U_1\cup U_2$ (see Figs. 3 and 14, for example).

Also, even though in Proposition III.4 and Theorem III.1 the range of η is restricted to $0<\eta<1$ (rather than $\eta>0$, $\eta\neq 2$), numerical experiments indicate that once η approaches $1-$, then trajectories become unbounded. Thus, it appears that no chaotic cases are lost if we restrict η, $0<\eta<1$.

Graphical methods, such as Lienard's (Ref. 10, pp. 31–33), have been found effective and useful in studying systems of nonlinear differential equations in 2D. To conclude this section, we describe a graphical method for the map $\mathcal{R}_0\mathcal{R}_1$. For any given point (v_1,v_2), we rewrite the relation (56) as

$$\begin{bmatrix}u_1\\u_2\end{bmatrix}=\frac{2+\eta}{2-\eta}\left\{\frac{\eta}{2+\eta}\begin{bmatrix}v_1\\F(v_2)\end{bmatrix}+\frac{2}{2+\eta}\begin{bmatrix}F(v_2)\\v_1\end{bmatrix}\right\}. \tag{64}$$

Note that in (64), the terms inside the curly parentheses are a convex combination of two points $(v_1,F(v_2))$ and $(F(v_2),v_1)$. Thus such a sum of terms corresponds to a point on the line segment with endpoints $(v_1,F(v_2))$ and $(v_2,F(v_1))$. Using (64), we show the graphical construction in Fig. 2 where C is the curve representing the function $v_1=F_{\alpha,\beta}(v_2)$, I is the point $(0,v_I)$, L_0 is the straight line $v_1=v_2$, P_0 is the point (v_1,v_2), P_1 is the point $(F(v_2),v_2)$, P_2 is the point

$(F(v_2),F(v_2))$, P_3 is the point $(v_1,F(v_2))$, P_4 is the point $(F(v_2),v_1)$, L_1 is the line segment joining P_3 with P_4, P_5 is a point on L_1 satisfying $P_5P_3{:}P_5P_4=\eta{:}2$, and P_6 is the image point (u_1,u_2) satisfying $OP_6{:}OP_5=(2+\eta)/(2-\eta)$.

IV. SNAPBACK REPELLERS AS A CAUSE OF CHAOS

Difficulties associated with proving chaos for noninvertible maps in two- or higher-dimensional spaces have been described itemwise in Secs. I A, B and C. As promised, we now focus our study on Sec. I B, the snapback repellers.

Snapback repellers for (noninvertible) one-dimensional maps are repelling fixed points with homoclinic orbits. The proof that they cause chaos may be found in Devaney (Ref. 11, Theorem 1.16.5, p. 124). We have found that that theorem can be properly generalized to N-dimensional noninvertible maps, and that for our 2D model problems under study here, such snapback repellers actually exist and, thus, they cause chaos. However, we are alerted by Ref. 9, p. 63, that a reference citation for snapback repellers by Marotto[9] already exists in the literature. It turns out that, however, by comparing Marotto's proof with ours, we are surprised that there is an error in Ref. 9. The error is not grievous; at his writing Marotto might think that it was just a simple fact (by changing to an equivalent norm to make things work) not worth mentioning at all. We nevertheless feel that the situation is confusing at least, leading us to clarify it below. We will then present a somewhat refined theorem in the spirit of Ref. 11, Theorem 1.16.5, *loc. cit.* (Even though the authors seem to have independently rediscovered such snapback repellers here, the credit of priority clearly goes to Marotto.[9])

First, recall the definition of a snapback repeller based on Marotto (Ref. 9, Def. 2.3, p. 203).

Definition IV.1: Let $\mathcal{F}{:}\mathbb{R}^N\to\mathbb{R}^N$ be C^1. Let Z be a fixed point of $\mathcal{F}$ such that all of the eigenvalues of $D\mathcal{F}(Z)$ have absolute values larger than 1. We say that Z is a snapback repeller if there exists a point X_0 in $W^u_{\rm loc}(Z)$, the local unstable set of Z, and some integer M, such that $\mathcal{F}^M(X_0)=Z$ and $\det D\mathcal{F}^M(X_0)\neq 0$. □

Now, let us restate the main theorem in Ref. 9.

Theorem IV.1: *[Marotto (Ref. 9, Theorem 3.1, pp. 204–205)] Let $\mathcal{F}{:}\mathbb{R}^N\to\mathbb{R}^N$ be C^1. If $\mathcal{F}$ possesses a snapback repeller, then $\mathcal{F}$ is chaotic. That is, there exists*

(i) a positive integer n such that for each integer $p\geqslant n$, $\mathcal{F}$ has a point of period p;

(ii) a ''scrambled set'' of $\mathcal{F}$, i.e., an uncountable set S containing no periodic points of $\mathcal{F}$ such that:

(a) $\mathcal{F}(S)\subset S$,

(b) for every $X,Y\in S$ with $X\neq Y$,

$$\overline{\lim_{k\to\infty}}|\mathcal{F}^k(X)-\mathcal{F}^k(Y)|>0,$$

(c) for every $X\in S$ and any periodic point Y of $\mathcal{F}$,

$$\overline{\lim_{k\to\infty}}|\mathcal{F}^k(X)-\mathcal{F}^k(Y)|>0;$$

(iii) an uncountable subset S_0 of S such that for every $X,Y\in S_0$,

$$\overline{\lim_{k\to\infty}}|\mathcal{F}^k(X)-\mathcal{F}^k(Y)|=0.$$

□

The statements in Theorem IV.1 are all correct without question. However, an error was made in the proof: in Ref. 9, p. 202, line 34, Marotto first states that in $\mathbb{R}^N$ that the usual Euclidean norm is to be used. Let us write it as

$$|x|_2=\left(\sum_{i=1}^N x_i^2\right)^{1/2},\quad \text{for } x=(x_1,\ldots,x_N)\in\mathbb{R}^N,$$

where the subscript 2 denotes the ℓ_2-norm. Then in Ref. 9, p. 203, lines 15–17, he writes:

''If all eigenvalues of $DF(Z)$ are greater than 1 in norm, then F displays the following local behavior at Z. For some $s>1$ and $r>0$:

$$\|F(X)-F(Y)\|>s\|X-Y\| \quad \text{for all } X,Y\in B_r(Z).'' \tag{65}$$

($B_r(Z)$ is the ball with radius r centered at Z.)

There, Marotto obviously was using the following property:

''Let A be an $N\times N$ real constant matrix such that all of its eigenvalues are larger than 1 in absolute value. Then A satisfies

$$|Ax|\geqslant\mu|x|, \quad \text{for some } \mu>1, \quad \text{for all } x\in\mathbb{R}^N.'' \tag{66}$$

Since in (65), the norm of Marotto's choice for the underlying space is the ℓ_2-norm, he must be interpreted to mean that in (66), there is a $\mu>1$ such that

$$|Ax|_2\geqslant\mu|x|_2, \quad \text{for all } x\in\mathbb{R}^N. \tag{67}$$

But it is well known that (67) is false. The following is a simple counterexample.

Example IV.1:Let ε and δ be positive. The matrix

$$A=\begin{bmatrix} 1+\epsilon+\dfrac{\delta}{2} & \dfrac{1}{2\delta} \\ \dfrac{\delta^3}{2} & 1+\epsilon+\dfrac{\delta}{2} \end{bmatrix}$$

has two eigenvalues $1+\epsilon$ and $1+\epsilon+\delta/2$, with respective corresponding eigenvectors

$$\begin{bmatrix} 1 \\ -\delta^2 \end{bmatrix}, \begin{bmatrix} 1 \\ \delta^2 \end{bmatrix}.$$

Choose a unit vector

$$x=\frac{1}{\sqrt{2}}\begin{bmatrix} 1 \\ -1 \end{bmatrix}.$$

Then

$$Ax=\frac{1}{\sqrt{2}}\begin{bmatrix} 1+\epsilon+\dfrac{\delta}{2}-\dfrac{1}{2\delta} \\ \dfrac{\delta^3}{2}-1-\epsilon-\dfrac{\delta}{2} \end{bmatrix}.$$

Take $\delta=1/2$. Then

$$|Ax|_2=\frac{1}{\sqrt{2}}\left[\left(\epsilon+\frac{1}{4}\right)^2+\left(1+\epsilon+\frac{3}{16}\right)^2\right]^{1/2}=\frac{1}{\sqrt{2}}\left[\frac{377}{256}+\epsilon\left(\frac{27}{8}+2\epsilon\right)\right]^{1/2}<0.9<1,$$

if ϵ is small. □

All norms in $\mathbb{R}^N$ or $\mathbb{C}^N$ are equivalent. What we need is a certain norm in $\mathbb{R}^N$ or $\mathbb{C}^N$ making (66) valid. We show, step by step, how to do this in the following.

Lemma IV 1: Let A be an invertible $N\times N$ real (resp. complex) constant matrix and let $|\ |$ be a norm in $\mathbb{R}^N$ (resp. $\mathbb{C}^N$). Then there exists a $\mu>0$ such that $|Ax|\geqslant\mu|x|$ holds for all $x\in\mathbb{R}^N$ (resp. $\mathbb{C}^N$) if and only if $\|A^{-1}\|\leqslant\mu^{-1}$, where $\|A^{-1}\|$ is the operator norm of A^{-1} corresponding to the norm $|\ |$ of the underlying $\mathbb{R}^N$ (resp. $\mathbb{C}^N$).

Proof: For any $x\in\mathbb{R}^N$ or $\mathbb{C}^N$, $x\neq 0$, we have

$$\mu^{-1}=\|A^{-1}\|=\sup_{y\neq 0}\frac{|A^{-1}y|}{|y|}\geqslant\frac{|A^{-1}w|}{|w|}=\frac{|x|}{|Ax|}\quad(x=A^{-1}w).$$

Therefore $|Ax|\geqslant\mu|x|$ for all $x\in\mathbb{R}^N$ or $\mathbb{C}^N$, $x\neq 0$, if and only if $\|A^{-1}\|\leqslant\mu^{-1}$. When $x=0$, the proof is trivial. □

Lemma IV.2: Let $D=\mathrm{diag}(\lambda_1,\ldots,\lambda_N)$ *be an* $N\times N$ *diagonal matrix with diagonal entries* $\lambda_1,\ldots,\lambda_N\in\mathbb{C}^N$. *Let* $\mathbb{C}^N$ *be the N-dimensional complex Euclidean space with* ℓ^2*-norm*

$$|z|_2=\left(\sum_{j=1}^{N}|z_j|^2\right)^{1/2},\quad z=(z_1,\ldots,z_N)\in\mathbb{C}^N.$$

Then $\|D\|_2$, *the operator norm of D corresponding to* $|\ |_2$, *satisfies*

$$\|D\|_2=\max_{1\leqslant j\leqslant N}|\lambda_j|.$$

Proof: Just expand any vector $z\in\mathbb{C}^N$ in terms of the basis eigenvectors $e_1,e_2,\ldots,e_n$, where e_j is the unit vector pointing in the jth axial direction. □

Lemma IV.3: Let J be an $m\times m$ *Jordan matrix with eigenvalue* λ *of Riesz index m:*

$$J=\begin{bmatrix}\lambda & 1 & 0 & \ldots & 0\\ 0 & \lambda & 1 & & \vdots\\ \vdots & & \ddots & \ddots & \\ \vdots & & & \ddots & 1\\ 0 & \ldots & 0 & & \lambda\end{bmatrix}.\tag{68}$$

Then for any given ε, *J has a similarity matrix* $\tilde{J}=D^{-1}JD$, *where D is an invertible diagonal matrix, such that*

$$\tilde{J}=\begin{bmatrix}\lambda & \varepsilon & & & 0\\ & \lambda & \varepsilon & & \\ & & \ddots & \ddots & \\ & & & \ddots & \varepsilon\\ 0 & & & & \lambda.\end{bmatrix}.\tag{69}$$

Proof: This can be found in Devaney (Ref. 11, Proposition 2.1.12, p. 168) or Franklin (Ref. 12, Exercise 13, p. 174). Its proof can be easily illustrated through the following 3×3 similarity matrix:

$$D^{-1}JD=\begin{bmatrix}a^{-1} & 0 & 0\\ 0 & a_2^{-1} & 0\\ 0 & 0 & a_3^{-1}\end{bmatrix}\begin{bmatrix}\lambda & 1 & 0\\ 0 & \lambda & 1\\ 0 & 0 & \lambda\end{bmatrix}\begin{bmatrix}a_1 & 0 & 0\\ 0 & a_2 & 0\\ 0 & 0 & a_3\end{bmatrix}=\begin{bmatrix}\lambda & a_1^{-1}a_2 & 0\\ 0 & \lambda & a_2^{-1}a_3\\ 0 & 0 & \lambda\end{bmatrix}.$$

Therefore, if we choose a_1,a_2, and a_3, the diagonal entries of D, to satisfy $a_1^{-1}a_2=a_2^{-1}a_3=\varepsilon$, we obtain the desired form (69). □

Theorem IV.2: Let A be an $N\times N$ *(real or complex) constant matrix such that all of its eigenvalues have absolute values larger than* μ. *Then there exists a norm* $|\cdot|$ *in* $\mathbb{C}^N$ *such that the associated operator-norm of* A^{-1}, $\|A^{-1}\|$, *satisfies* $\|A^{-1}\|\leqslant\mu^{-1}$. *Consequently, A satisfies* $|Ax|\geqslant\mu|x|$ *for all* $x\in\mathbb{R}^N$ *or* $\mathbb{C}^N$.

Proof: We first perform a similarity transformation to obtain $A^{-1}=PJP^{-1}$, where J is a Jordan canonical form of A^{-1}; J consists of submatrices J_k diagonally, for $k=1,2,\ldots,l$, where each J_k has the form (68). Applying Lemma IV.3, we may now assume that each J_k has the form

(69). Therefore, J is an ε-perturbation of a diagonal matrix; call that diagonal matrix D. The diagonal entries of D consist of λ_j^{-1}, the multiplicative inverses of the eigenvalues λ_j of A. By Lemma IV.2 and the assumption that $|\lambda_j|>\mu$ for all λ_j, we have

$$\|D\|_2=\max_j|\lambda_j^{-1}|<\mu^{-1}.$$

Since J is an ε-perturbation of D, for ε sufficiently small we obtain

$$\|J\|_2\leqslant\|D\|_2+\varepsilon'\leqslant\mu^{-1}, \tag{70}$$

because $\varepsilon'>0$ depends only on ε and can thus be made as small as we wish.

In $\mathbb{C}^N$, we now define a P-norm by

$$|z|_P=|P^{-1}z|_2.$$

Then, for a $z\in\mathbb{C}^N$,

$$|A^{-1}z|_P=|P^{-1}A^{-1}z|_2=|JP^{-1}z|_2\leqslant\|J\|_2|P^{-1}z|_2\leqslant\mu^{-1}|z|_P, \text{ by (70).}$$

Therefore

$$\|A^{-1}\|_P=\sup\frac{|A^{-1}z|_P}{|z|_P}\leqslant\mu^{-1}.$$

By Lemma IV.1, we have

$$|Ax|_P\geqslant\mu|x|_P, \quad \text{for all } x\in\mathbb{R}^N \quad \text{or } \mathbb{C}^N.$$

By incorporating Theorem IV.2 into its proof, Theorem IV.1 is now true. However, in what follows, let us provide a somewhat refined version of Theorem IV.1. Let

$$\mathcal{F}:\mathbb{R}^N\to\mathbb{R}^N, \quad \mathcal{F}(x)=(f_1(x),f_2(x),\ldots,f_N(x)), \quad x\in\mathbb{R}^N,$$

be a C^1 map. Then for $x^{(1)},x^{(2)}\in\mathbb{R}^N$, by applying the mean value theorem to the scalar-valued functions $f_1,\ldots,f_N$, we have

$$\mathcal{F}(x^{(1)})-\mathcal{F}(x^{(2)})=(\nabla f_1(y^1)\cdot(x^{(1)}-x^{(2)}),\nabla f_2(y^2)\cdot(x^{(1)}-x^{(2)}),\ldots,\nabla f_N(y^N)\cdot(x^{(1)}-x^{(2)})), \tag{71}$$

for some $y^1,\ldots,y^N\in\mathbb{R}^N$, where each y^j lies on the open line segment $L=\{y\in\mathbb{R}^N|y=\alpha x^{(1)}+(1-\alpha)x^{(2)},\alpha\in(0,1)\}$. We write (71) as

$$\mathcal{F}(x^{(1)})-\mathcal{F}(x^{(2)})=\mathcal{D}F\cdot[x^{(1)}-x^{(2)}], \tag{72}$$

where $\mathcal{DF}=\mathcal{DF}(Y)$, with $Y=(y^1,\ldots,y^n)\in\mathbb{R}^{N\times N}$, is an $N\times N$ matrix whose ith row vector is $\nabla f_i(y^i)$, where $\nabla f_i(y^i)$ makes (71) satisfied.

Theorem IV.3: Let $\mathcal{F}:\mathbb{R}^N\to\mathbb{R}^N$ be C^1, and p be a snapback repeller of $\mathcal{F}$. Then for each neighborhood U of p, there is an integer $n>0$ such that $\mathcal{F}^n$ has a hyperbolic invariant subset in U on which $\mathcal{F}^n$ is topologically conjugate to the shift map on the binary symbol space Σ_2.

Proof: The argument goes the same way as that in Ref. 11, Theorem 1.16.5, p. 124. Since p is a snapback repeller, all of the eigenvalues of $D\mathcal{F}(p)$ have absolute values larger than 1. By Theorem IV.2, we can define a norm $|\cdot|$ on $\mathbb{R}^N$ such that $\|[D\mathcal{F}(p)]^{-1}\|\leqslant\mu^{-1}$, for some $\mu>1$. By continuity, we can find an open neighborhood W of p in U and some $\tilde{\mu},1<\tilde{\mu}<\mu$, such that

$$\|[\mathcal{DF}(Y)]^{-1}\|\leqslant\tilde{\mu}^{-1}, \quad \text{for all } Y=(y^1,\ldots,y^N)\in W^N. \tag{73}$$

By the assumption of a snapback repeller, we can take a point $q\in W$ such that $\mathcal{F}^n(q)=p$ and $\det(D(\mathcal{F}^n)(q))\neq0$. Since the orbit of q contains only a finite number of points that do not lie in

W, and since $\det(D\mathcal{F}^n(q))\neq 0$, by continuity we can find a neighborhood V of q in W such that $\mathcal{DF}^n(Y)$ is invertible for all $Y=(y^1,\ldots,y^N)\in V^N$. Therefore there exists some $\varepsilon>0$ such that

$$\|[\mathcal{DF}^n(Y)]^{-1}\|<\varepsilon^{-1}, \quad \text{for all } Y=(y^1,\ldots,y^N)\in V^N. \tag{74}$$

From the invertibility of $\mathcal{DF}^n(Y)$, we see that $\mathcal{F}^n$ maps V diffeomorphically onto an open set $\mathcal{F}^n(V)$ containing p in its interior.

We now choose j so that $(\tilde{\mu}^j\varepsilon)^{-1}<1$. We choose V sufficiently small so that $\mathcal{F}^{n+i}(V)\subset W$, but $\mathcal{F}^{n+i}(V)\cap V=\varnothing$, for $i=1,2,\ldots,j$. Since $V\subset W$, from (72), (73), and Lemma IV.1, for $k>j$ and for any two points $x^1,x^2\in V$, we have

$$\begin{aligned}
|\mathcal{F}^{n+k}(x^1)-\mathcal{F}^{n+k}(x^2)| &= |\mathcal{F}^{n+k}(x^1)-\mathcal{F}^{n+k}(x^2)| \\
&= |\mathcal{DF}(Y^1)\cdot(\mathcal{F}^{n+k-1}(x^1)-\mathcal{F}^{n+k-1}(x^2))| \\
&\geqslant \tilde{\mu}|\mathcal{F}^{n+k-1}(x^1)-\mathcal{F}^{n+k-1}(x^2)| \quad (\text{where } Y^1\in W^N) \\
&= \tilde{\mu}|\mathcal{DF}(Y^2)\cdot(\mathcal{F}^{n+k-2}(x^1)-\mathcal{F}^{n+k-2}(x^2))| \quad (\text{where } Y^2\in W^N) \\
&\geqslant \tilde{\mu}^2|\mathcal{F}^{n+k-2}(x^1)-\mathcal{F}^{n+k-2}(x^2)| \\
&\geqslant \cdots \\
&\geqslant \tilde{\mu}^k|\mathcal{F}^n(x^1)-\mathcal{F}^n(x^2)| = \tilde{\mu}^k|\mathcal{DF}^n(Y^k)\cdot(x^1-x^2)| \quad (\text{where } Y^k\in V^N) \\
&\geqslant \tilde{\mu}^k\varepsilon|x^1-x^2| \geqslant \tilde{\mu}^{k-j}|x^1-x^2|.
\end{aligned}$$

Therefore $\mathcal{F}^{n+k}$ expands V and for k sufficiently large, $\mathcal{F}^{n+k}(V)$ covers V. We have a diffeomorphism $\mathcal{F}^{n+k}:V\to\mathcal{F}^{n+k}(V)$ such that $p\in\mathcal{F}^{n+k}(V)$ and $V\subset\mathcal{F}^{n+k}(V)$.

Let us choose a sufficiently small open subset V' containing $(\mathcal{F}^{n+k})^{-1}(V)$. By choosing V sufficiently small and k large, we can make V' satisfy

(i) $V\cap V'=\varnothing$;
(ii) $\mathcal{F}^{n+k}(V)\supset V\cup V'$;
(iii) $\mathcal{F}^{n+k}(V')\supset V$;
(iv) $\mathcal{F}^{n+k}(V')\subset W$;
(v) $\mathcal{F}^{n+k}$ is a strict expansion on V'.

Therefore the map $\mathcal{F}^{n+k}$ has a shift sequence

$$V'\to V\to V'\cup V,$$

where each member (except the leader) of the sequence is covered by the image of the predecessor. Therefore $\mathcal{F}^{n+k}(V'\cup V)\supset V'\cup V$, and $V'\cup V$ has an invariant subset

$$\Lambda\equiv\{x\in V'\cup V|(\mathcal{F}^{n+k})^j(x)\in V'\cup V, j=0,1,2,\ldots\}.$$

For any $x\in\Lambda$ we define its binary (itinerary) symbol as

$$s(x)=(s_0s_1s_2\ldots s_j\ldots), \quad s_j=0 \text{ if } (\mathcal{F}^{n+k})^jx\in V', \quad s_j=1 \text{ if } (\mathcal{F}^{n+k})^jx\in V.$$

Then it is a standard procedure to show that $\mathcal{F}^{n+k}$ is topologically conjugate to the shift automorphism on Σ_2, the space of all binary symbols. The proof is complete. □

Note that all consequences (i), (ii), and (iii) in Marotto's Theorem IV.1 can be deduced from the symbolic dynamics implied by Theorem IV.3.

Remark IV.1: In verifying the snapback repeller assumption in order to be able to apply Theorem IV.3, one needs to check the following conditions according to Definition IV.1:

(i) p is a fixed point of $\mathcal{F}$ such that all eigenvalues of $D\mathcal{F}(p)$ have absolute values larger than 1; (75)
(ii) there exists a $q\in W^u_{\text{loc}}(p)$ such that $\mathcal{F}^M(q)=p$ for some positive integer M; (76)
(iii) $\det D\mathcal{F}^M(q)\neq 0$. (77)

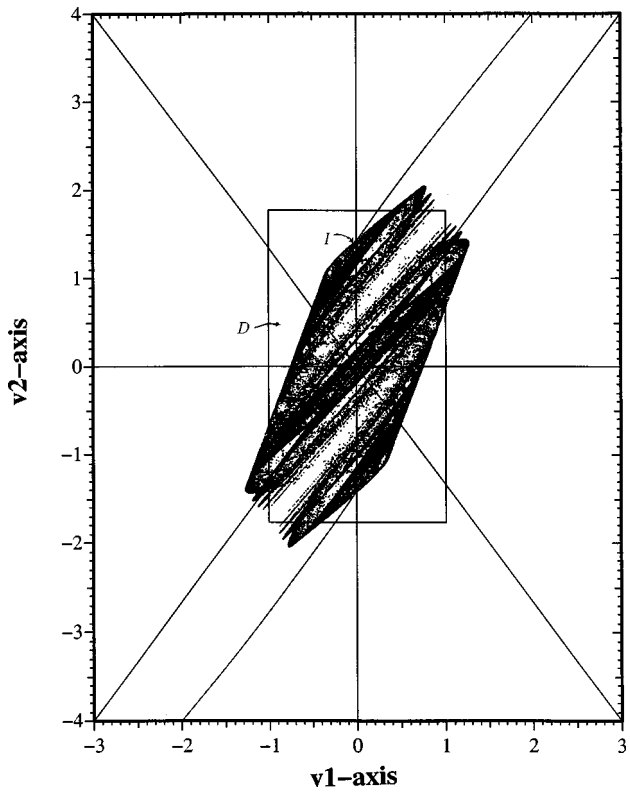

FIG. 3. The strange attractor for Example V.1, where $\alpha=0.9980$, $\beta=1$, and $\eta=0.7570$ are used. D represents the region defined by (54). The origin lies inside the ''cloud'' and, thus, is a snapback repeller.

In most cases, the verification work must be done through the aid of a computer, which automatically involves numerical errors. The verification of (i) is easiest, and the computer result can be trusted with total confidence. To verify (ii), one needs to do computer-aided search of *preimages* of p and then check whether such preimages can wind up in $W^u_{\rm loc}(p)$. This kind of reverse search can easily accumulate large numerical errors. Therefore, the value of M, even if computable in principle, would *not be entirely trustworthy*. Nevertheless, using the *continuity property of* $\mathcal{F}$, one can still conclude whether such an M (and, consequently, a homoclinic orbit) *exists or not*.

The verification of (iii) is the *most difficult* in general, because as we just pointed out in the above paragraph, it is very difficult to pin down an accurate value of M. Even if M is firmly determined, checking whether $\det D\mathcal{F}^M(q)\neq 0$ is still generally *impossible* because the evaluation of $D\mathcal{F}^M(q)$ usually involves computer roundoff errors. On the one hand, using the holomorphic property of the map $\mathcal{F}$ with respect to the parameter(s), one may claim that there exist at least some parameter values such that (4.13) holds for some snapback homoclinic orbit. On the other hand, we can expect, ''almost beyond reasonable doubt,'' that even if (77) fails, i.e., $\det D\mathcal{F}^M(q)=0$, there should still be chaos. The situation $\det D\mathcal{F}^M(q)=0$ signifies *degeneracy* and leads us to believe that what we have is a *degenerate (snapback) homoclinic orbit*. According to our knowledge of 1D maps, degenerate homoclinic orbits actually causes perhaps the *strongest chaos*.[11] This leads us to pose a conjecture below:

Conjecture: Let $\mathcal{F}:\mathbb{R}^N\to\mathbb{R}^N$ be C^1 satisfying (75) and (76). Then there exists a hyperbolic invariant subset of $W^u_{\rm loc}(p)$ on which $\mathcal{F}^n$ on Λ is topologically conjugate to the shift map on Σ_2. □

V. NUMERICAL EXAMPLES

We provide two examples in this section. Throughout, we fix $\beta=1$.

Example V.1: The origin as a snapback repeller of $\mathcal{R}_0\mathcal{R}_1$. For α, $0<\alpha\leqslant 1$, we know that the origin (0,0) is a repelling fixed point by Proposition III.2.

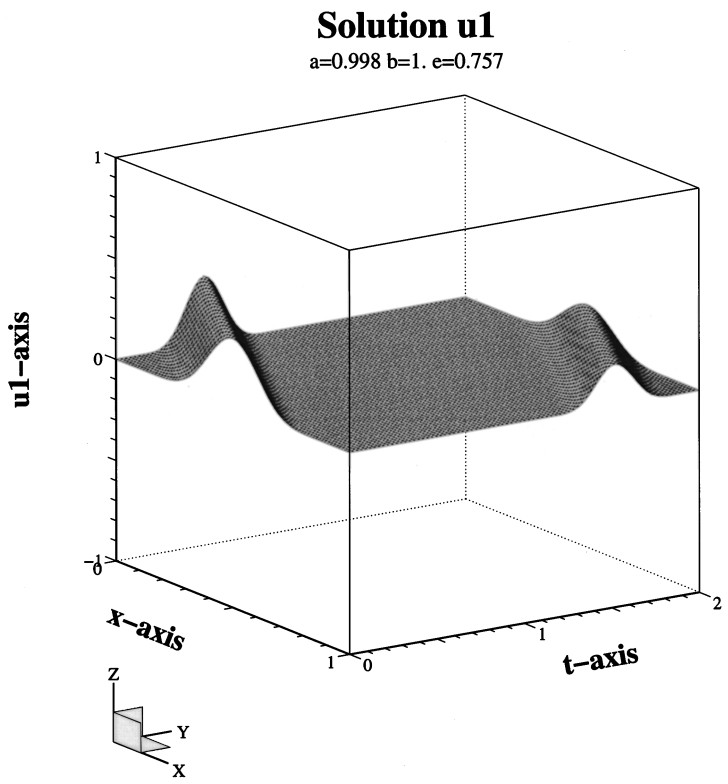

FIG. 4. The spatiotemporal profile of u_1 for initial time duration $[0,\ 2]$.

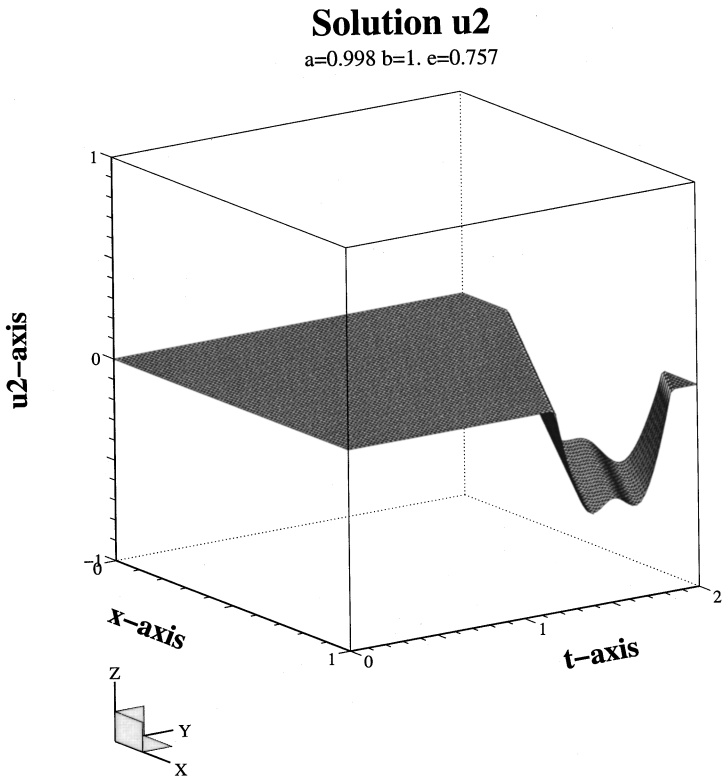

FIG. 5. The spatiotemporal profile of u_2 for initial time duration $[0,\ 2]$.

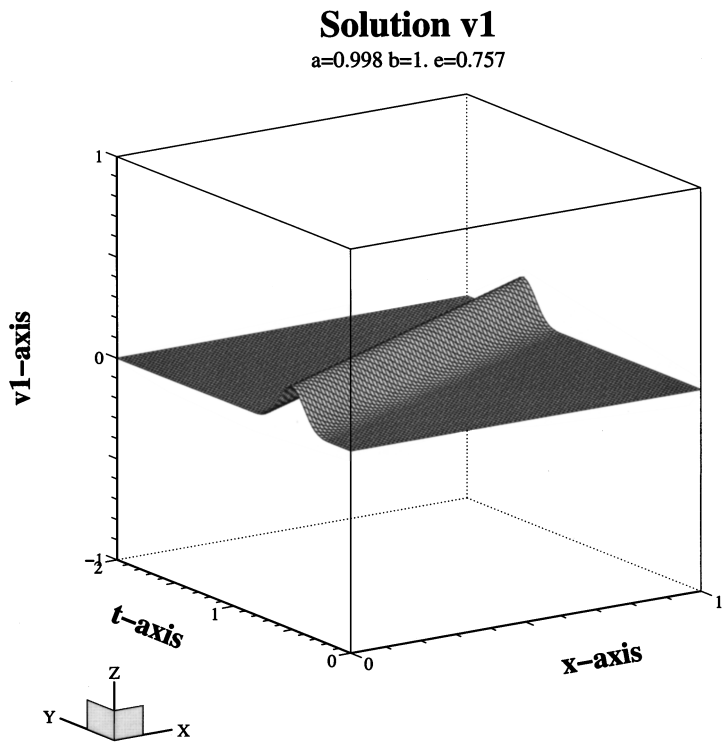

FIG. 6. The spatiotemporal profile of v_1 for initial time duration $[0,\ 2]$.

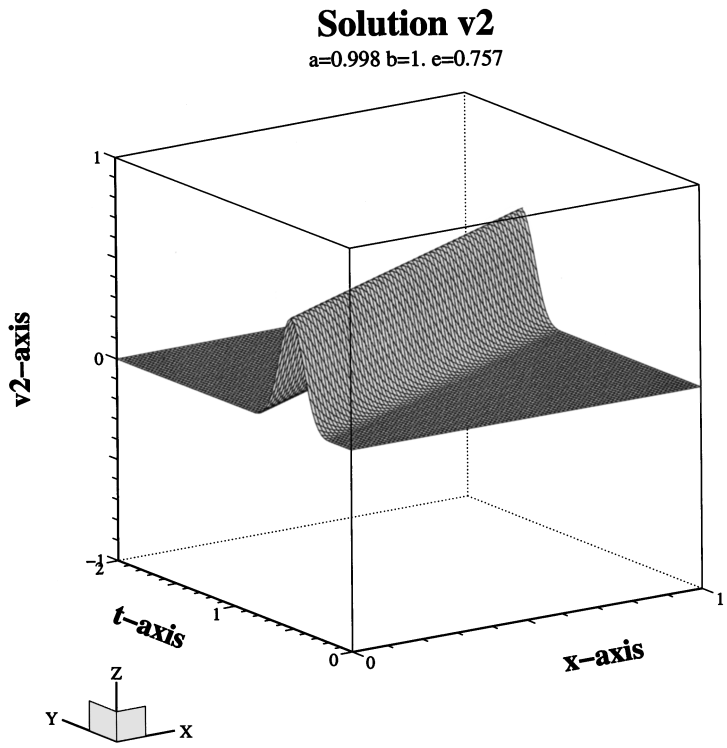

FIG. 7. The spatiotemporal profile of v_2 for initial time duration $[0,\ 2]$.

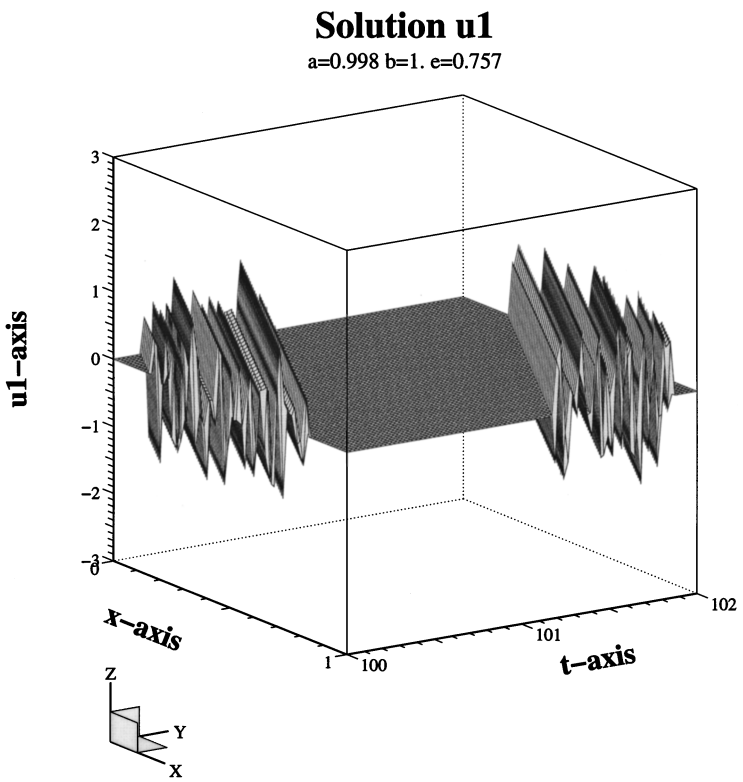

FIG. 8. The spatiotemporal profile of u_1 for time duration [100, 102].

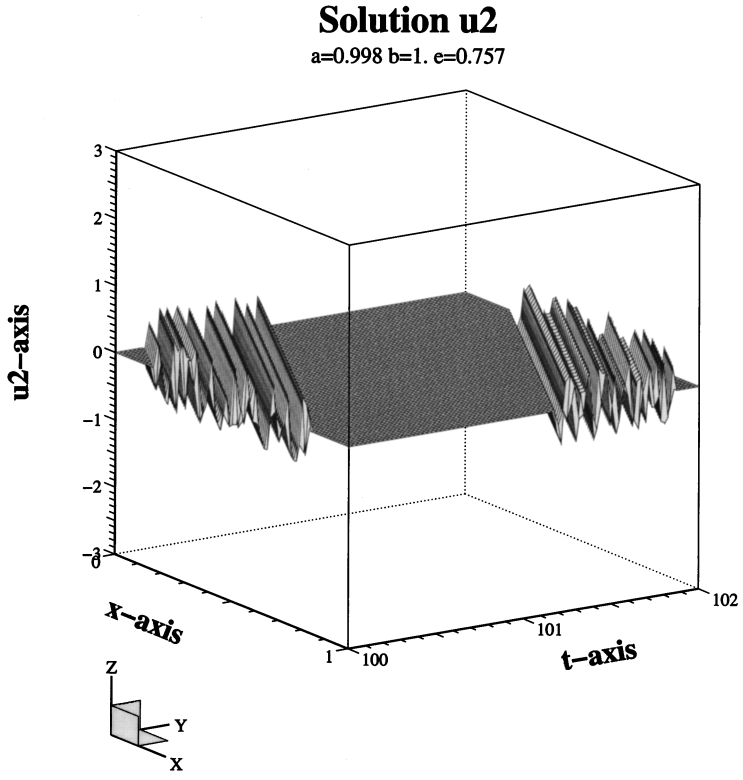

FIG. 9. The spatiotemporal profile of u_2 for time duration [100, 102].

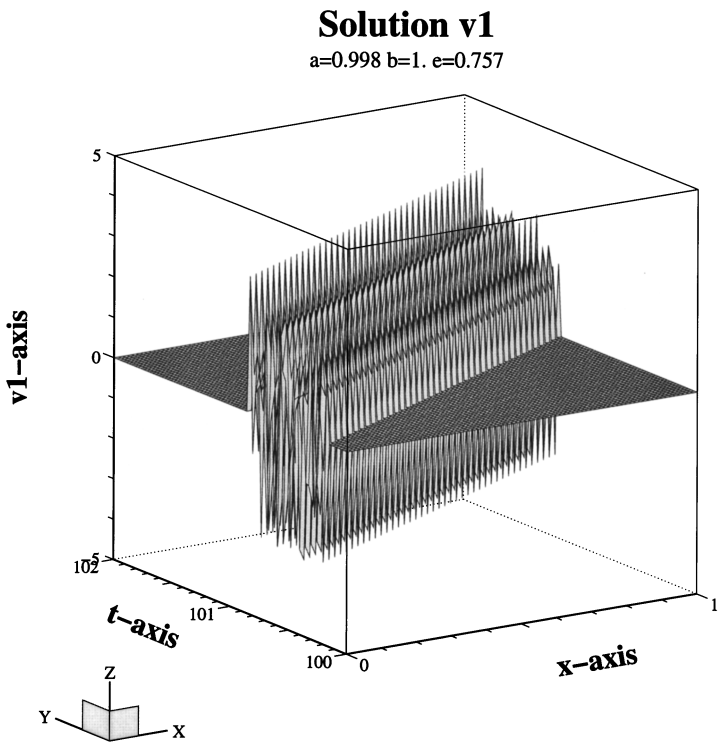

FIG. 10. The spatiotemporal profile of v_1 for time duration [100, 102].

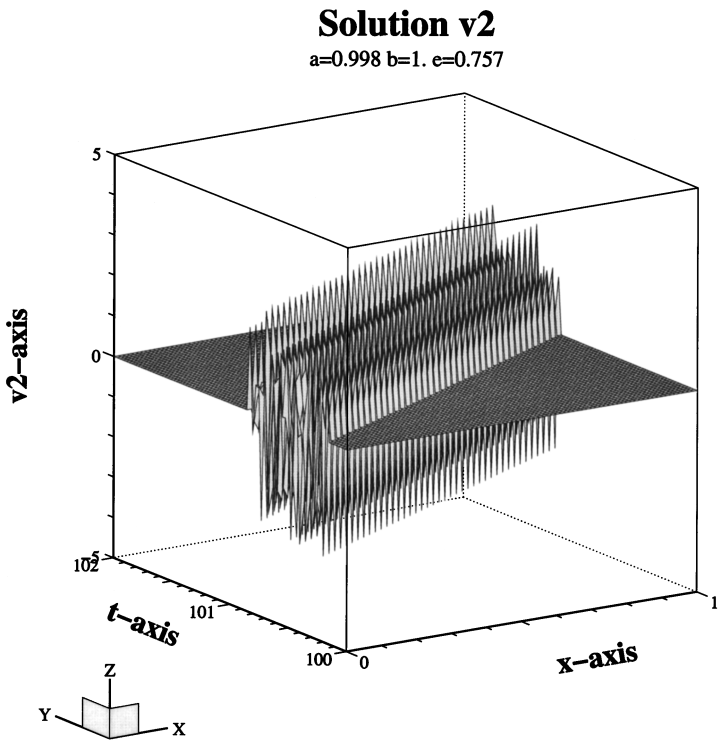

FIG. 11. The spatiotemporal profile of v_2 for time duration [100, 102].

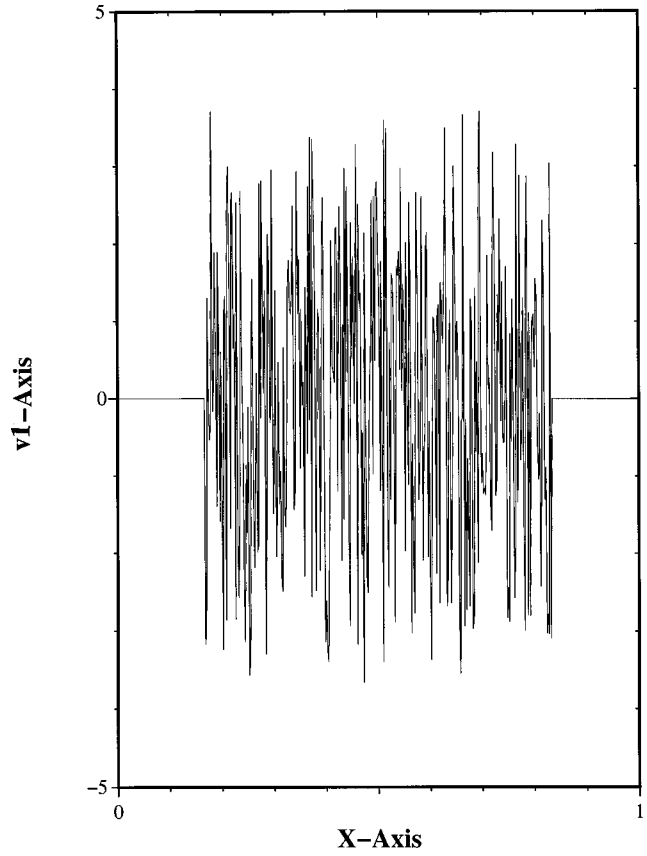

FIG. 12. The snapshot of v_1 at time $t=101$.

Through many numerical experiments, we have found that the origin will not be a snapback repeller unless α is close to 1.

We choose $\alpha=0.9980$, $\beta=1$, and $\eta=0.7570$. To see whether there is a strange attractor, we plot the iterates

$$(\mathcal{R}_0\mathcal{R}_1)^k P_0, \quad P_0=(0.005,0.005), \quad 10^4\leqslant k\leqslant 10^5.$$

What we obtain is a ''cloud,'' the strange attractor, as shown in Fig. 3. Note that the point $I=(0,v_I)$ (cf. Fig. 2) is mapped into the origin:

$$(\mathcal{R}_0\mathcal{R}_1)I=(0,0),$$

and in Fig. 3, I is ''hidden in the cloud.'' Therefore, by Remark IV.1, the continuity of $\mathcal{R}_0\mathcal{R}_1$ implies that the origin is a snapback repeller, i.e., (76) is satisfied. The verification of (77) is difficult, however, as noted in Remark IV.1. We have made no attempts to verify it.

To see chaotic vibration, we consider the system (15)–(18), with the initial data

$$u_{1,0}(x)=\frac{1}{12}\cdot\begin{cases}(x-x_1)^3/h^3, & x_1\leqslant x\leqslant x_2,\\ 1+\dfrac{3(x-x_2)}{h}+\dfrac{3(x-x_2)^2}{h^2}-\dfrac{3(x-x_2)^3}{h^3}, & x_2\leqslant x\leqslant x_3,\\ 1-\dfrac{3(x-x_4)}{h}+\dfrac{3(x-x_4)^2}{h^2}+\dfrac{3(x-x_4)^3}{h^3}, & x_3\leqslant x\leqslant x_4,\\ (x_5-x)^3/h^3, & x_4\leqslant x\leqslant x_5\\ 0, & \text{elsewhere,}\end{cases} \tag{78}$$

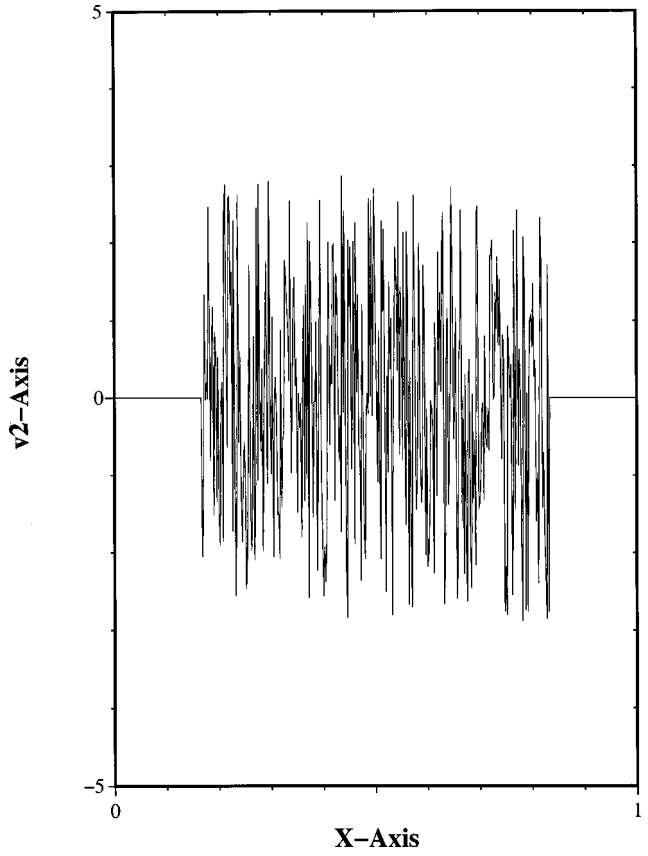

FIG. 13. The snapshot of v_2 at time $t=101$.

$$h=1/6, \quad x_j=j/6, \quad \text{for } j=1,2,3,4,5;$$
$$u_{2,0}(x)=v_{1,0}(x)=v_{2,0}(x)\equiv 0, \quad 0\leqslant x\leqslant 1. \tag{79}$$

Note that the function given in (78) is a C^2-continuous smoothest spline of degree 3. The initial data (78) and (79) satisfy the boundary conditions (16) and (18). It is not difficult to show (by mimicking the proof in Ref. 3, Theorem 6.1 that the system has a unique C^2-solution (u_1,u_2,v_1,v_2) on $(x,t)\in[0,1]\times[0,\infty)$.

The spatiotemporal profiles of u_1,u_2,v_1,v_2 are displayed, respectively, in Figs. 4, 5, 6, and 7 for the first two time units, i.e., $t\in[0,2]$.

For time $t\in[100,102]$, the spatiotemporal profiles of u_1,u_2,v_1,v_2 are displayed, respectively, in Figs. 8, 9, 10, and 11.

The snapshots at $t=101$ of v_1 and v_2 are displayed, respectively, in Figs. 12 and 13. We do not need to display u_1 and u_2 at $t=101$ because u_1 and u_2 are identically zero.

These profiles are computed by using the explicit representation formulas (20). Note that because of the *nondispersive* effects of wave propagation, all components u_1,u_2,v_1, and v_2 of the system can display a ''totally serene'' (i.e., zero or no disturbance) zone right next to the chaotic spatiotemporal region. □

Example V.2: A period-4 point as a snapback repeller of $(\mathcal{R}_0\mathcal{R}_1)^4$. Let us choose $\alpha=0.6$, $\beta=1$, and $\eta=0.8200$.

The map $\mathcal{R}_0\mathcal{R}_1$ has a strange attractor as shown in Fig. 10, suggesting that $\mathcal{R}_0\mathcal{R}_1$ is chaotic. Note in Fig. 14 that neither the point I nor the origin lies inside the strange attractor ''cloud;'' in this case, we can easily rule out the origin as a snapback repeller.

The map $\mathcal{R}_0\mathcal{R}_1$ has many period-4 orbits. So let us compute the fixed points of $(\mathcal{R}_0\mathcal{R}_1)^4$ by Newton's method. We have obtained three sets of such orbits (80), (82), and (84) and other relevant data as given below:

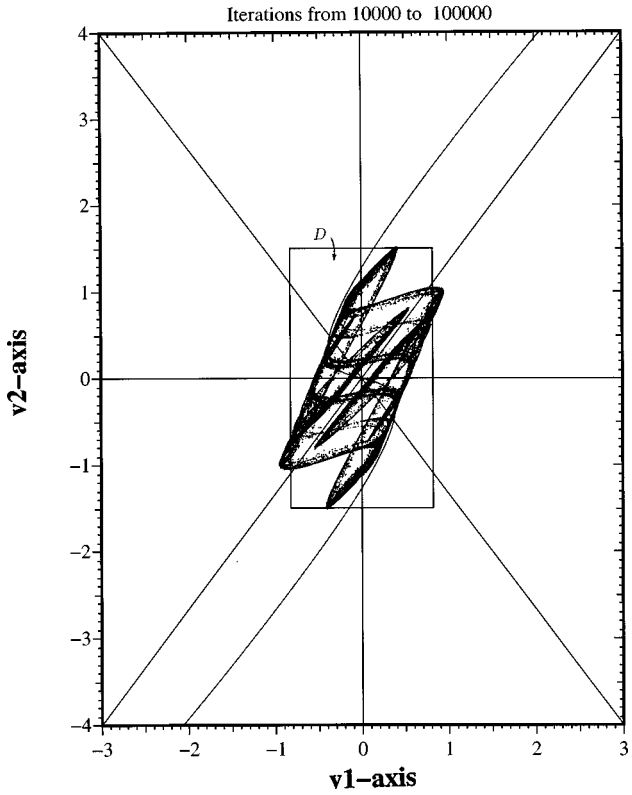

FIG. 14. The strange attractor for Example V.2, where $\alpha=0.6$, $\beta=1$, and $\eta=0.82$ are used. D is the rectangle defined by (54). Note that the origin is not inside the ''cloud'' of the strange attractor.

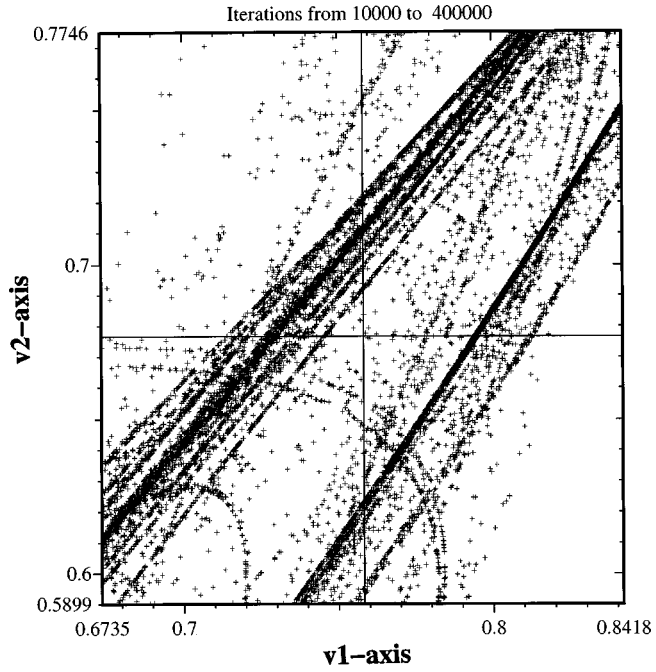

FIG. 15. This is a zoom-in of the vicinity of the period-4 point $P_1^{(1)}=(0.7582,\ 0.6762)$, cf. (80), from Fig. 14. Note that $P_1^{(1)}$is highlighted as the intersection of the horizontal and vertical lines near the center of the figure. Chaos in the immediate vicinity of $P_1^{(1)}$ is not strong.

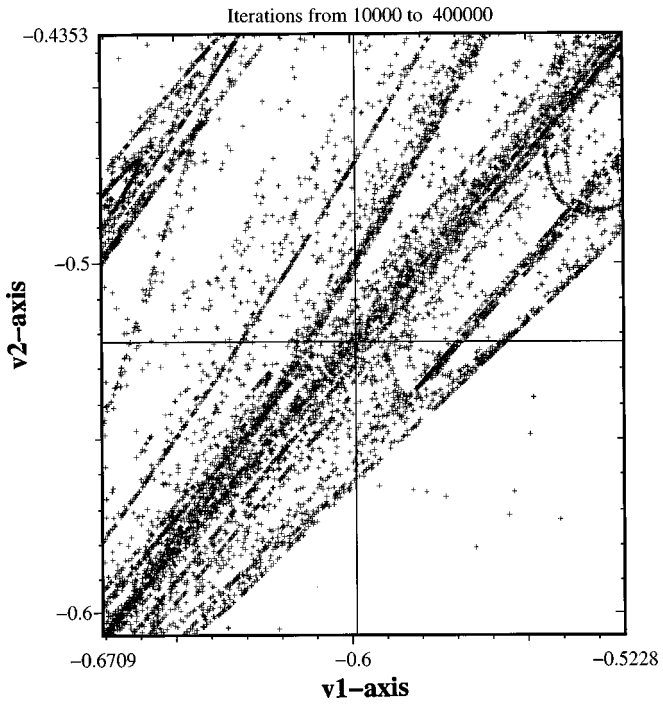

FIG. 16. This is a zoom-in of the vicinity of the period-4 point $P_2^{(1)}=(-0.5988,\ -0.5229)$, cf. (81), from Fig. 14. Note that $P_2^{(1)}$ is highlighted as the intersection of the horizontal and vertical lines near the center of the figure. Chaos is strong in the immediate vicinity of $P_2^{(1)}$.

$$\text{(i)}\quad \begin{cases} P_1^{(1)}=(0.7582,\quad 0.6762), \quad P_1^{(2)}=(2.1507,\quad 1.0699), \\ P_1^{(3)}=(-0.1942,\quad -7.6573), \quad P_1^{(4)}=(0.2591,\quad -0.1675); \end{cases} \tag{80}$$

$$D((\mathcal{R}_0\mathcal{R}_1)^4)(P_1^{(1)})=\begin{bmatrix} -4.4737 & -1.9625 \\ -8.2024 & -5.7953 \end{bmatrix},\ \text{with eigenvalues } -9.2007 \text{ and } -1.0683. \tag{81}$$

$$\text{(ii)}\quad \begin{cases} P_2^{(1)}=(-0.5988,\ -0.5229), \quad P_2^{(2)}=(0.1968,\ -0.7636), \\ P_2^{(3)}=(0.5988,\ 0.5229), \quad P_2^{(4)}=(-0.1968,\ 0.7636); \end{cases} \tag{82}$$

$$D((\mathcal{R}_0\mathcal{R}_1)^4(P_2^{(1)}))=\begin{bmatrix} 3.9208 & 1.2102 \\ 4.4494 & 1.4967 \end{bmatrix},\quad \text{with eigenvalues } 0.0908 \text{ and } 5.3267. \tag{83}$$

$$\text{(iii)}\quad \begin{cases} P_3^{(1)}=(-0.4492,\ -0.0324), \quad P_3^{(2)}=(-0.1076,\ -0.6774), \\ P_3^{(3)}=(0.4492,\ 0.0324), \quad P_3^{(4)}=(0.1076,\ 0.6774). \end{cases} \tag{84}$$

$$D((\mathcal{R}_0\mathcal{R}_1)^4(P_3^{(1)}))=\begin{bmatrix} -6.1730 & 44.6753 \\ -13.7347 & 90.5629 \end{bmatrix},\quad \text{with eigenvalues } 0.6515,\ 83.7384. \tag{85}$$

Note that $P_i^{(j)}$ satisfies

$$(\mathcal{R}_0\mathcal{R}_1)^k(P_i^{(j)})=P_i^{((k+j)\bmod 4)},\quad i=1,2,3.$$

Let us now zoom in on Fig. 10 about these period-4 points $P_1^{(1)}, P_2^{(1)}$, and $P_3^{(1)}$ (see Figs. 15, 16, and 17, respectively.)

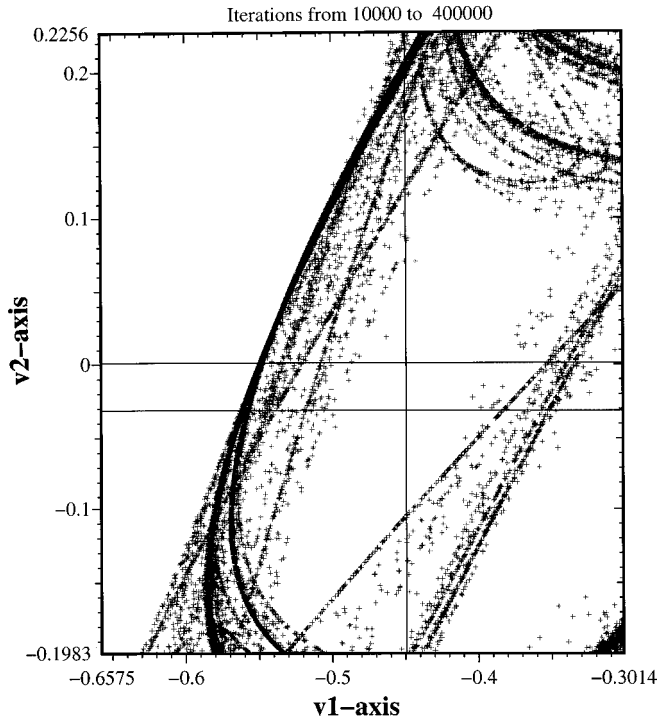

FIG. 17. This is a zoom-in of the vicinity of the period-4 point $P_3^{(1)}=(-0.4492,\ -0.0324)$, cf. (84), from Fig. 14. This point is not inside the ''cloud'' of the strange attractor; it does not have a homoclinic orbit. There is no chaos in the close vicinity of $P_3^{(1)}$.

From (81) and Fig. 15, by the continuity argument as given in Remark IV.1, it is quite clear that with $\mathcal{F}=(\mathcal{R}_0\mathcal{R}_1)^4$, the point $P_1^{(1)}$ satisfies (75) and (76). Thus, $P_1^{(1)}$ ''should be'' a snapback repeller. However, we observe in Fig. 15 that *chaos is not strong in the immediate vicinity of* $P_1^{(1)}$.

From (83) and Fig. 16, we see that $P_2^{(1)}$ is a saddle node fixed point $(\mathcal{R}_0\mathcal{R}_1)^4$ with a homoclinic orbit. *Chaos is very strong in the immediate vicinity of* $P_2^{(1)}$.

From (85), we note that $P_3^{(1)}$ is again a saddle node fixed point of $(\mathcal{R}_0\mathcal{R}_1)^4$. However, $P_3^{(1)}$ is not on the strange attractor, as can be seen from Fig. 17, suggesting that $P_3^{(1)}$ does not have a homoclinic orbit. *There is no chaos at all in the immediate vicinity of* $P_3^{(1)}$.

This example suggests the following:

(1) Snapback repellers imply chaos, but its strength may not be strong when other sources of chaos are present.
(2) A saddle node fixed point having a (forward) homoclinic orbit seems to cause strong chaos, even without the diffeomorphism assumption.

Point (2) above appears particularly important. We hope to be able to report some results in the future. □

ACKNOWLEDGMENTS

G.C. and J.Z. were supported in part by NSF Grant DMS No. 96-10076, Texas Advanced Research Program Grant No. 010366-046, and Texas A&M University Grant No. 96-36. S.B.H. was supported in part by a grant from the National Council of Science of the Republic of China.

[1] G. Chen, H. B. Hsu, and J. Zhou, ''Linear superposition of chaotic and orderly vibrations on two serially connected strings with a van der Pol joint,'' Int. J. Bifurcation Chaos Appl. Sci. Eng. **6**, 1509–1527 (1996).
[2] G. Chen, H. B. Hsu, and J. Zhou, ''Chaotic vibration of the one-dimensional wave equation due to a self-excitation boundary condition, Part I: controlled hysteresis,'' Transactions Amer. Math. Soc. (to appear).
[3] G. Chen, H. B. Hsu, and J. Zhou, ''Chaotic vibration of the one-dimensional wave equation due to a self-excitation

boundary condition, Part II: energy injection, period doubling and homoclinic orbit,'' Int. J. Bifurcation Chaos Appl. Sci. Eng. **8**, 423–445 (1998).
[4] G. Chen, H. B. Hsu, and J. Zhou, ''Chaotic vibration of the one-dimensional wave equation due to a self-excitation boundary condition, Part III: natural hysteresis memory effects,'' Int. J. Bifurcation Chaos Appl. Sci. Eng. **8**, 447–470 (1998).
[5] G. Chen and J. Zhou, *Vibration and Damping in Distributed Systems, Vol. I, Analysis, Estimation, Attenuation and Design* (CRC, Boca Raton, FL, 1994).
[6] K. S. Liu, F. L. Huang, and G. Chen, ''Exponential stability analysis of a long chain of coupled vibrating strings with dissipative linkage,'' SIAM (Soc. Ind. Appl. Math.) J. Appl. Math. **49**, 1694–1707 (1989).
[7] S. Wiggins, *Introduction to Applied Nonlinear Dynamical Systems and Chaos* (Springer-Verlag, New York, 1990).
[8] C. Mira, L. Gardini, A. Barugola, and J. C. Cathala, *Chaotic Dynamics in Two-Dimensional Noninvertible Maps* (World Scientific, Singapore, 1996).
[9] F. R. Marotto, ''Snap-back repellers imply chaos in $\mathbb{R}^n$,'' J. Math. Anal. Appl. **63**, 199–223 (1978).
[10] J. J. Stoker, *Nonlinear Vibrations* (Wiley, New York, 1950).
[11] R. L. Devaney, *An Introduction to Chaotic Dynamical Systems*, 2nd ed. (Addison–Wesley, New York, 1989).
[12] J. Franklin, *Matrix Theory* (Prentice–Hall, Englewood Cliffs, NJ, 1968).